https://doi.org/10.5194/bg-2021-149
Preprint. Discussion started: 10 June 2021

Biogeosciences Discussions Open Access EGU

Biogeochemical controls on wintertime ammonium accumulation in the surface layer of the Southern Ocean

Shantelle Smith[1*], Katye E. Altieri[1], Mhlangabezi Mdutyana[1,2], David R. Walker[3], Ruan G. Parrott[1], Kurt A.M. Spence[1], Jessica M. Burger[1], Sarah E. Fawcett[1,4]

[1] Department of Oceanography, University of Cape Town, Private Bag X3, Rondebosch, Cape Town, South Africa
[2] Southern Ocean Carbon and Climate Observatory (SOCCO), CSIR, Rosebank, Cape Town, South Africa
[3] Department of Conservation and Marine Sciences, Cape Peninsula University of Technology, Cape Town, South Africa
[4] Marine and Antarctic Research centre for Innovation and Sustainability (MARIS), University of Cape Town, Cape Town, South Africa

[*] Corresponding author: smtsha023@myuct.ac.za

1. Abstract

The production and consumption of ammonium (NH_4^+) are essential upper-ocean nitrogen cycle pathways, yet in the Southern Ocean where NH_4^+ has been observed to accumulate in surface waters, its mixed-layer cycling remains poorly understood. For surface samples collected between Cape Town and the marginal ice zone (MIZ) in winter 2017, we found that NH_4^+ concentrations were five-fold higher than is typical for summer, and lower north than south of the Subantarctic Front (SAF; 0.01–0.26 µM versus 0.19–0.70 µM). Our observations confirm that NH_4^+ accumulates in the Southern Ocean's winter mixed layer, particularly in polar waters. NH_4^+ uptake rates were highest near the Polar Front (PF; 12.9 ± 0.4 nM day^{-1}) and in the Subantarctic Zone (10.0 ± 1.5 nM day^{-1}), decreasing towards the MIZ (3.0 ± 0.8 nM day^{-1}) despite high ambient NH_4^+ concentrations, likely due to low sea surface temperatures and light availability. By contrast, rates of NH_4^+ oxidation were higher south than north of the PF (16.0 ± 0.8 versus 11.1 ± 0.5 nM day^{-1}), perhaps due to the lower light and higher iron conditions characteristic of polar waters. Augmenting our dataset with NH_4^+ concentration measurements spanning the 2018/2019 annual cycle reveals that mixed-layer NH_4^+ accumulation south of the SAF likely derives from sustained heterotrophic NH_4^+ production in late summer through winter that outpaces NH_4^+ consumption by temperature-, light, and iron-limited microorganisms. Our observations thus imply that the Southern Ocean becomes a biological source of CO_2 to the atmosphere for half the year not only because nitrate drawdown is weak, but also because the ambient conditions favour net heterotrophy and NH_4^+ accumulation.

2. Introduction

The Southern Ocean impacts the Earth system through its role in global thermohaline circulation, which drives the exchange of heat and nutrients among ocean basins (Frolicher et al., 2015; Popp et al., 1999; Sarmiento et al., 2004). The Southern Ocean also plays an integral

https://doi.org/10.5194/bg-2021-149
Preprint. Discussion started: 10 June 2021

role in mediating climate, by transferring carbon to the deep ocean via its biological and solubility pumps (Sarmiento & Orr, 1991; Volk & Hoffert, 1985) and through the release of deep-ocean CO_2 to the atmosphere during deep-water ventilation (i.e., CO_2 leak; Broecker & Peng, 1992; Lauderdale et al., 2013; Sarmiento & Toggweiler, 1984). Upper Southern Ocean circulation is dominated by the eastward-flowing Antarctic Circumpolar Current (ACC) that consists of a series of broad circumpolar bands ("zones") separated by oceanic fronts. Southern Ocean fronts can drive water mass formation (Ito et al., 2010) and nutrient upwelling that supports elevated biological activity (Longhurst, 1998; Sokolov & Rintoul, 2007).

Concentrations of the essential macronutrients, nitrate (NO_3^-) and phosphate (PO_4^{3-}), are perennially high in Southern Ocean surface waters, in contrast to most of the global ocean. Consumption of these nutrients, and thus primary productivity in the Southern Ocean, is limited by numerous (often overlapping) factors, including temperature, light, micronutrient concentrations, and grazing pressure (e.g., Boyd et al., 2001; Martin et al., 1990; Reay et al., 2001; Smith Jr & Lancelot, 2004). These limitations vary with Southern Ocean sector (i.e., longitude), zone (i.e., latitude), and season, resulting in spatial and seasonal variations in chlorophyll-a concentrations, primary production, plankton community composition, and nutrient uptake regime (Shadwick et al., 2015; Thomalla et al., 2011; Mengesha et al., 1998; Mdutyana et al., 2020). For example, the Antarctic Zone (AZ; see Text S1 for definitions of zones and fronts), which includes the Open and Polar Antarctic Zones (OAZ and PAZ, respectively), is characterized by sparser phytoplankton populations than the Polar Frontal Zone (PFZ; Mengesha et al., 1998) even though AZ spring blooms generally host higher diatom abundances than the blooms of the Subantarctic Zone (SAZ) and PFZ (Kopczyńska et al., 2007). In addition to the seasonal cycles of temperature and light, Southern Ocean ecosystems are influenced by seasonal changes in nutrient availability. In winter, deep mixing replenishes the nutrients required for phytoplankton growth but the low temperatures and light levels impede biological activity (Rintoul & Trull, 2001). Once the mixed layer shoals in spring and summer, phytoplankton begin to consume the available nutrients until some form of limitation (usually iron; Mtshali et al., 2019; Nelson et al., 2001) sets in. This balance between wintertime nutrient recharge and summertime nutrient drawdown is central to the role of the Southern Ocean in setting atmospheric CO_2 (Sarmiento & Toggweiler, 1984).

Iron limitation, which sets in following the spring/early summer bloom, causes phytoplankton to increase their dependence on recycled ammonium (NH_4^+; Timmermans et al., 1998), which has a far lower iron requirement than NO_3^- assimilation (Price et al., 1994). The extent to which phytoplankton rely on NO_3^- versus NH_4^+ as their primary N source has implications for Southern Ocean CO_2 removal since phytoplankton growth fuelled by upwelled NO_3^- ("new production") must be balanced on an annual basis by the export of sinking organic matter ("export production"; Dugdale & Goering, 1967), which drives CO_2 sequestration (i.e., the biological pump; Volk & Hoffert, 1985). By contrast, phytoplankton growth on NH_4^+ or other recycled N forms ("regenerated production") yields no net removal of CO_2 to the deep ocean (Dugdale & Goering, 1967; Eppley & Peterson, 1979). To-date, considerable research has focused on NO_3^- cycling in the Southern Ocean mixed layer because of the importance of this nutrient for the biological pump (e.g., DiFiore et al., 2006; Francois et al., 1992; Johnson et al., 2017; Mdutyana et al., 2020; Primeau et al., 2013; Sarmiento & Toggweiler, 1984; Sigman & Boyle, 2000) and global ocean fertility (Sarmiento et al., 2004). By contrast, the active cycling

https://doi.org/10.5194/bg-2021-149
Preprint. Discussion started: 10 June 2021

of regenerated N within the seasonally-varying mixed layer – including the production of NH_4^+ and its consumption by phytoplankton uptake and nitrification (the microbial oxidation of NH_4^+ to nitrite (NO_2^-) and then NO_3^-) – remains poorly understood.

NH_4^+ is produced in the euphotic zone as a by-product of heterotrophic metabolism (i.e., ammonification; Herbert, 1999) and as a consequence of grazing by zooplankton (Lehette et al., 2012; Steinberg & Saba, 2008), and is removed by phytoplankton uptake (in euphotic waters) and nitrification (mainly in aphotic waters). Heterotrophic bacteria can also directly consume NH_4^+ (Kirchman, 1994) and have been hypothesized to do so at significant rates in the Southern Ocean mixed layer in winter (Cochlan, 2008; Mdutyana et al., 2020). NH_4^+ assimilation by phytoplankton, in contrast to NO_3^- consumption, requires relatively little energy (Dortch, 1990) such that NH_4^+ is usually consumed in the surface ocean as rapidly as it is produced (Glibert, 1982; La Roche, 1983), resulting in very low open-ocean NH_4^+ concentrations (<0.2 µM; Paulot et al., 2015). Additionally, NH_4^+ is often the preferred N source to phytoplankton communities dominated by smaller species, while larger phytoplankton such as diatoms that invest more energy in nutrient consumption specialize in the assimilation of NO_3^- (e.g., Chisholm, 1992; Fawcett & Ward, 2011). Phytoplankton communities typically shift towards smaller species when iron and/or light are limiting (Pearce et al., 2010; Tagliabue et al., 2014; Deppeler & Davidson, 2017), since a higher cellular surface area-to-volume ratio renders small phytoplankton less vulnerable to diffusion limitation (Hudson & Morel, 1993; Mei et al., 2009) and a larger cell volume limits light absorption efficiency (Finkel et al., 2004; Fujuki & Taguchi, 2002).

In addition to the consequences for small versus large phytoplankton abundance, which has implications for the organic matter sinking flux (i.e., the strength of the biological pump; Alldredge & Gotschalk, 1988; Richardson & Jackson, 2007) and higher trophic levels (e.g., Venkataramana et al., 2019), determining the dominant N source to phytoplankton provides a means of estimating their potential for CO_2 removal, as per the new production paradigm (Dugdale & Goering, 1967). The N isotopic composition ($\delta^{15}N$, in ‰ vs. N_2 in air, = $(^{15}N/^{14}N_{sample}/^{15}N/^{14}N_{air} - 1) \times 1000$) of particulate organic N (PON) can be used to infer the dominant N source to phytoplankton (Altabet, 1988; Lourey et al., 2003; Fawcett et al., 2011; Van Oostende et al. 2017) since the assimilation of subsurface NO_3^- yields PON that is higher in $\delta^{15}N$ than that fuelled by recycled NH_4^+ (the $\delta^{15}N$ of which is inferred from isotopic fractionation associated with its production to be low) (Macko et al. 1986; Silfer et al. 1992; Checkley & Miller, 1989; Sigman et al, 1999). The $\delta^{15}N$ of bulk PON yields an integrated view of the autotrophic N uptake regime (Fawcett et al., 2011; 2014; Lourey et al., 2003), which can be complicated by overlapping processes such as bacterial degradation of organic matter (Möbius, 2013; Smart et al., 2020). By contrast, ^{15}N tracer-derived N uptake rates provide an instantaneous measure of the extent of phytoplankton reliance on new versus regenerated N (Lipschultz, 2008), although these rates can be poorly-suited to extrapolation.

Nitrification was historically considered unimportant in euphotic zone waters due to the evidence for light inhibition of nitrifiers (Hooper & Terry, 1974; Horrigan & Springer, 1990; Olson, 1981; Schön & Engel, 1962) and competition with phytoplankton for NH_4^+ (Smith et al., 2014; Ward, 1985; 2005; Zakem et al., 2018). However, this view has been challenged in numerous oceanic regions (Yool et al., 2007) including the Southern Ocean (Smart et al., 2015;

https://doi.org/10.5194/bg-2021-149
Preprint. Discussion started: 10 June 2021

Cavagna et al., 2015; Fripiat et al., 2015), with elevated rates of NH_4^+ oxidation recently observed throughout the winter mixed layer in all major Southern Ocean zones (Mdutyana et al., 2020). Wintertime upper-ocean NH_4^+ dynamics thus have implications for annual estimates of carbon export potential, insofar as NO_3^- produced by nitrification in the winter mixed layer that is subsequently supplied to spring/summer phytoplankton communities constitutes a regenerated rather than a new source of N on an annual basis (Yool et al., 2007; Mdutyana et al., 2020).

Surface concentrations of NH_4^+ and other reduced N forms are often near-zero in spring and early/mid-summer in the open Southern Ocean (Daly et al., 2001; Sambrotto & Mace, 2000; Savoye et al., 2004; Henley et al., 2020) as NH_4^+ is readily consumed by phytoplankton. In late summer, a peak in NH_4^+ concentration has been observed and attributed to enhanced bacterial and zooplankton activity following elevated phytoplankton growth (Mengesha et al., 1998; Becquevort et al., 2000; Dennett et al., 2001; Sambrotto & Mace, 2000; El-Sayed, 1984). One might expect this high-concentration NH_4^+ pool to be quickly consumed given the capacity of phytoplankton for rapid NH_4^+ uptake, leaving the winter mixed layer NH_4^+-deplete. However, the limited available observations suggest that wintertime surface NH_4^+ concentrations are high (often >1 µM), particularly south of the Subantarctic Front (SAF) (Bianchi et al., 1997; Philibert et al., 2015; Mdutyana et al., 2020; Henley et al., 2020). If ambient NH_4^+ is not depleted following the late summer peak in its concentration despite the high rates of NH_4^+ uptake and oxidation measured in autumn and winter (Bianchi et al., 1997; Thomalla et al., 2011; Philibert et al., 2015; Mdutyana et al., 2020), then NH_4^+ regeneration must be occurring at an elevated rate, either coincident with NH_4^+ consumption in winter and/or prior to this in late summer and/or autumn. Under these conditions, the Southern Ocean mixed layer may become net heterotrophic and thus a biological source of CO_2 to the atmosphere.

Here, we focus on NH_4^+ cycling in the Southern Ocean mixed layer in winter, a season assumed to be largely biologically dormant (Arrigo et al., 2008; Schaafsma et al., 2018) and for which NH_4^+ cycle data are scarce. We confirm that NH_4^+ accumulates throughout the winter mixed layer, particularly south of the SAF, and examine a number of potential causes thereof, including a contribution from the residual late-summer NH_4^+ pool, sustained NH_4^+ production in the autumn/winter, and limited NH_4^+ uptake and/or oxidation in winter. We further consider the possible drivers and implications of each of these scenarios. Finally, using NH_4^+ concentration data collected over a full annual cycle, we propose a seasonal cycle for the mixed-layer NH_4^+ pool south of the SAF.

3. Methods

3.1 Cruise track and sample collection

Samples were collected on the southward (S) and northward (N) legs of a winter cruise between Cape Town, South Africa, and the marginal ice zone (MIZ) of the Southern Ocean onboard the R/V *SA Agulhas II* (VOY25; 28 June to 13 July 2017) (Fig. 1). Leg S, involving only surface underway collections, crossed the Atlantic sector of the Southern Ocean, while leg N bordered the Atlantic and Indian sectors (30°E; WOCE IO6 line) and involved eight conductivity-temperature-depth (CTD) hydrocast stations. Frontal positions were determined

https://doi.org/10.5194/bg-2021-149
Preprint. Discussion started: 10 June 2021

using the ship's hull-mounted thermosalinograph and supported by temperature, salinity, and oxygen concentration data from CTD measurements made during leg N. The criteria for determining frontal positions included identifying sharp gradients in potential temperature, salinity, potential density, and oxygen concentrations (Belkin & Gordon, 1996; Lutjeharms & Valentine, 1984; Orsi et al., 1995). For leg N, the mixed layer depth (MLD) was determined for each Niskin (up)cast as the depth between 10 m and 400 m at which the Brunt Väisälä Frequency squared, N^2, reached a maximum (Carvalho et al., 2017).

During leg S, samples were collected every four hours from the ship's underway system (~7 m intake; "underway stations") while samples on leg N were collected from surface (~10 m) Niskin bottles mounted on the CTD rosette ("CTD stations"). NH_4^+ samples were also taken at 13 depths over the upper 500 m at all CTD stations. At all stations (underway + CTD), ~40 mL of unfiltered seawater was collected for the analysis of NH_4^+ concentrations in duplicate 50 mL high density polyethylene (HDPE) bottles that had been stored ("aged") with orthophthaldialdehyde (OPA) working reagent. Unfiltered seawater was collected in 50 mL polypropylene centrifuge tubes for the analysis of macronutrients including urea. Immediately following collection, NH_4^+ and nutrient samples were stored at -20°C.

Duplicate size-fractionated chlorophyll-a samples were collected by filtering seawater (500 mL) through 25 mm-diameter glass fibre filters with pore sizes of 0.3 µm and 2.7 µm (Sterlitech, GF-75 and Grade D, respectively). Acetone was added to foil-wrapped borosilicate test tubes containing the filters that were then incubated at -20 °C for 24 hours. Additionally, duplicate seawater samples (4 L) were gently vacuum-filtered through combusted 47 mm-diameter, 0.3 µm-pore size GF-75 filters for POC and PON concentrations and δ^{15}N-PON. Filters were stored in combusted foil envelopes at -80°C.

For microscopy, unfiltered seawater samples (250 mL) were collected along leg S in darkened glass bottles and immediately fixed by the addition of 2.5 mL of Lugol's iodine solution (2% final concentration), then stored at low room temperature away from direct sunlight until analysis. Surface seawater samples (~2 mL) were collected in triplicate microcentrifuge tubes for flow cytometry. These samples were fixed with glutaraldehyde (1% final concentration) and stored at -80°C until analysis (Marie et al., 2005; Vaulot et al., 1989).

Ten incubation experiments were conducted during leg S to measure the rate of net primary production (NPP). NH_4^+ and chlorophyll-a samples were collected at the beginning of each experiment as described above. In addition, four NPP experiments were conducted during leg N using seawater collected from Niskin bottles fired at 10 m. In all cases, pre-screened (using 200-µm mesh to remove large grazers) seawater was collected in three 2-L polycarbonate bottles to which $NaH^{13}CO_3$ was added at ~5% of the ambient DIC concentration. Bottles were incubated on the deck for 5 to 6.5 hours in custom-built incubators shaded with neutral-density screens to mimic the 55% light level (typically encountered between 5 and 10 m) and supplied with running surface seawater. Following incubation, each sample was divided (1 L per size fraction) and gently vacuum filtered through 0.3 µm, and 2.7 µm glass fibre filters that were stored in combusted foil at -80°C until analysis.

https://doi.org/10.5194/bg-2021-149
Preprint. Discussion started: 10 June 2021

N uptake (as NO_3^-, NH_4^+ and urea) and NH_4^+ oxidation experiments were conducted at five stations during leg S, with NH_4^+ oxidation measured at two additional stations at the ice edge (Fig. 1). On leg N, experiments were also conducted using seawater collected from 10 m at the same four CTD stations as the NPP experiments. In all cases, duplicate polycarbonate bottles were amended with ^{15}N-labeled NO_3^-, NH_4^+ or urea at ~10% of the ambient N concentration, estimated based on past wintertime measurements (Mdutyana et al., 2020) and, in the case of NH_4^+, coincident shipboard analyses. Incubations were carried out as described above for NPP. For NH_4^+ oxidation, duplicate black 250 mL HDPE bottles were amended with 0.1 µM $^{15}NH_4^+$ and 0.1 µM $^{14}NO_2^-$ (the latter as a "trap" for the $^{15}NO_2^-$ produced by NH_4^+ oxidation given the expected low ambient NO_2^- concentrations (<0.2 µM; Zakem et al., 2018; Fripiat et al., 2019; Mdutyana et al., 2020). NH_4^+ oxidation bottles were incubated for 24 hours under the same temperature conditions as the N uptake and NPP experiments. Subsamples (50 mL) were collected from each bottle immediately following the addition of $^{15}NH_4^+$+$^{14}NO_2^-$ (T_0) and at the end of the experiments (T_f), and frozen at -20°C until analysis.

3.2. Sample processing

3.2.1. Ammonium concentrations

NH_x ($NH_4^+ + NH_3$) concentrations were measured shipboard following the fluorometric method of Holmes et al. (1999) and using a Turner Designs Trilogy fluorometer 7500-000 equipped with a UV module. The detection limit, calculated as twice the pooled standard deviation of all standards, was 0.06 µM. NH_x is hereafter referred to as NH_4^+ given convention in the oceanographic literature and the dominance of NH_4^+ over NH_3 at seawater pH. To prevent possible in/efflux of contaminant ammonia (NH_3) due to the temperature difference between winter surface waters and the shipboard laboratory, samples were frozen immediately upon collection and OPA working reagent was subsequently added to the frozen samples prior to defrosting them for analysis. Samples were slowly warmed to room temperature in a water bath after OPA addition, incubated in the dark for four hours once defrosted, then analysed in triplicate. Standards and blanks were made daily using Type-1 ultrapure Milli-Q water. Precision was ± 0.03 µM for replicate samples and standards.

3.2.2. Macronutrient concentrations

Following the cruise, duplicate seawater samples were analysed manually for NO_2^- and PO_4^{3-} (Bendschneider & Robinson, 1952; Murphy & Riley, 1962) using a Thermo Scientific Genesys 30 Visible spectrophotometer. Standards and blanks were prepared in Type-1 ultrapure Milli-Q water. Precision was ± 0.05 µM for NO_2^- and ± 0.06 µM for PO_4^{3-}, and the detection limit for NO_2^- and PO_4^{3-} was 0.05 µM. NO_3^-+NO_2^- and $Si(OH)_4$ concentrations were measured in duplicate using a Lachat QuickChem 8500 Series 2 flow injection autoanalyzer. Aliquots of a certified reference material (JAMSTEC) were measured during each run to ensure measurement accuracy (SD ≤ 2%). The precision of the NO_3^-+NO_2^- and $Si(OH)_4$ measurements was ± 0.4 µM and ± 0.2 µM, respectively, and the detection limit was 0.1 µM and 0.2 µM. The NO_3^- concentration was calculated by subtraction (i.e., [NO_3^-+NO_2^-] – [NO_2^-]), with error propagated according to standard statistical practices. Urea-N (hereafter, urea) concentrations were determined according to the room-temperature, single-reagent colorimetric

https://doi.org/10.5194/bg-2021-149
Preprint. Discussion started: 10 June 2021

method (Revilla et al., 2005) using a Thermo Scientific Genesys 30 Visible spectrophotometer; precision was ± 0.04 µM and the detection limit was 0.04 µM.

3.2.3. Chlorophyll-a concentrations

Chlorophyll-a concentrations ([chl-a]) were determined shipboard using the nonacidified fluorometric method (Welschmeyer, 1994). The fluorometer was calibrated with an analytical standard (*Anacystis nidulans*, Sigma-Aldrich®) prior to and following the cruise. The [chl-a] of the 0.3-2.7 µm size class (picophytoplankton) was calculated by subtracting the measured [chl-a] of the >2.7 µm size class (nanophytoplankton) from the >0.3 µm size class (bulk). We assumed based on previous work (e.g., Hewes et al., 1985, 1990; Weber & El-Sayed, 1987) that the wintertime phytoplankton community would be composed primarily of small cells (i.e., typically <10 µm), such that we did not separate micro- from nanophytoplankton.

3.2.4. Bulk POC, PON and δ^{15}N-PON

The NPP and N uptake filters were fumed with hydrochloric acid in a desiccator for 24 hours to remove inorganic C, then dried for 24 hours at 40°C and packaged in tin cups. Filters to be measured for δ^{15}N were dried in the same way as the NPP/N uptake filters, but not acidified. Samples were analysed using a Delta V Plus isotope ratio mass spectrometer (IRMS) coupled to a Flash 260 elemental analyser, with a detection limit of 0.17 µmol C and 0.07 µmol N and precision of ±0.005 At% for C and N. Eight unused pre-combusted filters (blanks) were prepared with each batch run of ~88 samples. POC and PON content was determined from daily standard curves of IRMS area versus known C and N masses. For isotope ratios, sample measurements were standardised to Merck Gel (δ^{15}N = 7.5‰, δ^{13}C = -20.1‰; Merck), Valine (δ^{15}N = 12.1‰, δ^{13}C = -26.8‰; Sigma), Choc (δ^{15}N = 4.3‰, δ^{13}C = -17.8‰), and NH_4Cl (δ^{15}N = -0.6‰), internal laboratory standards calibrated against IAEA reference materials.

3.2.5. Size-fractionated rates of NPP and N uptake

Carbon and N uptake rates (NPP, ρNH_4^+, ρNO_3^-, ρUrea) were calculated according to the equations outlined in Dugdale & Wilkerson (1986) as:

$$\rho M = \frac{[PM]\ x\ (At\%_{meas} - At\%_{amb})}{T\ x\ (At\%_{init} - At\%_{amb})} \quad \text{(Eqn 1)}$$

$$\text{where, } At\%_{init} = \frac{([M]\ x\ At\%_{amb}) + ([M_{tracer}]\ x\ At\%_{tracer})}{[M] + [M_{tracer}]} \quad \text{(Eqn 2)}$$

Here, M is the species of interest (C, NH_4^+, NO_3^-, or urea); ρM is the uptake rate of that species (nM day^{-1}); [PM] is the concentration of POC or PON (µM) on the filters; [M] is the ambient concentration of DIC, NH_4^+, NO_3^-, or urea at the time of sample collection; [M_{tracer}] is the concentration of $NaH^{13}CO_3$, $^{15}NH_4^+$, $^{15}NO_3^-$, or ^{15}N-urea added to the incubation bottles; and T is the incubation period (days). The PM and ρM of the picoplankton size class was calculated by subtracting the >2.7 µm-filter measurements (i.e., nanoplankton) from the >0.3 µm-filter (i.e., bulk) measurements.

https://doi.org/10.5194/bg-2021-149
Preprint. Discussion started: 10 June 2021

The specific carbon fixation rate (V_C) was calculated as ρC/POC and the specific uptake rate of total N (V_{Ntot}) was calculated as ρN_{tot}/PON (where $\rho N_{tot} = \rho NH_4^+ + \rho NO_3^- + \rho Urea$). The f-ratio (Eppley & Peterson, 1979), used to estimate the fraction of NPP potentially available for export, was then calculated as:

$$f-ratio = \frac{V_{NO_3}}{V_{NO_3} + V_{NH_4} + V_{urea}} \quad \text{(Eqn 3)}$$

No urea uptake experiments were conducted at the underway stations at 50.7ºS and 55.5ºS (both AZ); here, the f-ratio was calculated omitting V_{urea}. For the other AZ stations at which urea uptake was measured, including V_{urea} decreased the fraction of new-to-total production by only 4-8% compared to f-ratio calculations based on V_{NO3} and V_{NH4}.

3.2.6. Ammonia oxidation rates

The azide method of McIlvin and Altabet (2005) was used to convert NO_2^- deriving from NH_4^+ oxidation to N_2O gas that was measured using a Delta V Plus IRMS with a custom-built purge-and-trap front end (McIlvin & Casciotti, 2011). This configuration yields a detection limit of 0.2 nmol N with a $\delta^{15}N$ precision of ± 0.1‰. The $\delta^{15}N$ of NO_2^- was derived from $^{45}N_2O/^{44}N_2O$ and the rate of NH_4^+ oxidation ($NH_4^+{}_{ox}$; nM day^{-1}) was calculated following Peng et al. (2015) as:

$$NH_4^+{}_{ox} = \frac{\Delta(^{15}NO_2^-)}{f_{NH_4}^{15} \times T} \quad \text{(Eqn 4)}$$

Here, $\Delta(^{15}NO_2^-)$ is the change in the concentration of $^{15}NO_2^-$ (nM) between the start and end of the incubation, calculated as the difference in the measured $\delta^{15}N$ of NO_2^- between the T_f and T_0 samples, $f_{NH_4}^{15}$ is the fraction of the NH_4^+ substrate labelled with ^{15}N at the start of the incubation, and T is the incubation length (days). All $^{15}NO_2^-$ produced during the incubations was assumed to derive from $^{15}NH_4^+$ oxidation. The detection limit ranged from 0.02 to 0.11 nM day^{-1}, calculated according to Santoro et al. (2013) and Mdutyana et al. (2020).

3.2.7 Plankton community composition

Microphytoplankton and microzooplankton groups (>5-10 µm) were identified and counted in a subsample (20 mL) from each 250 mL amber bottle using the Utermöhl technique (Utermöhl, 1958) and following the recommendations of Hasle (1978). Plankton groups and individual species were counted and identified using an inverted light microscope (Olympus CKX41) at 200x magnification.

Cells were also enumerated using an LSR II flow cytometer (BD Biosciences) equipped with blue, red, violet, and green lasers. Here, our focus was on enumerating pico- and nanoplankton. Prior to flow cytometric analysis, 1 mL of each sample was incubated with 10 µL of 1% (v/v) SYBR Green-I, which stains DNA, at room temperature in the dark for 10 minutes (Marie et al., 1997). Autofluorescence was detected in the following bandpass filter sets, named for commonly-used fluorochromes: allophycocyanin (APC, 660/20), R-phycoerythrin (PE) (575/25), fluorescein isothiocyanate (FITC) (525/20), PE-cyanine 7 (PE-Cy7) (780/40), PE-

https://doi.org/10.5194/bg-2021-149
Preprint. Discussion started: 10 June 2021

Texas Red (610/20), and Pacific Blue (450/50). Background 'noise' was gated out based on the forward and side light scatter values (FSC = 800 and SSC = 200). DNA-containing cells were isolated in each sample based on their detected autofluorescence on the FITC bandpass filter (above a minimal fluorescence threshold of $x10^3$ RFU). Subsequently, based on their detected autofluorescence on the APC bandpass filter relative to the PE bandpass filter, the isolated DNA-containing cells were grouped into the following populations: Nano- and picoeukaryotes, and *Synechococcus*. Additionally, small heterotrophic cells were identified as containing DNA but with the lowest detected autofluorescence across all bandpass filters, except the FITC (Marie et al., 1997; Gasol & Del Giorgio, 2000). All particles lacking DNA were considered detritus. For each sample, data acquisition was terminated when a minimum of 5000 and maximum of 10000 events were recorded. The populations of interest were gated using FlowJo 10.3 software (TreeStar, Inc.; www.flowjo.com). Relative cell sizes were determined using 60 µL of SPHERO™ Blank Calibration Particles, 1.8 – 2.2 µm in diameter, added to 1 mL of selected samples to yield a final concentration of ~$6x10^5$ particles mL^{-1}. Relative to the 1.8 – 2.2 µm calibration beads, nanoeukaryotes were larger than 2.2 µm, picoeukaryotes and heterotrophic cells were smaller than 1.8 µm, and *Synechococcus* exhibited a range of sizes around 2 µm, with two distinct subgroups; one of ~2 µm in size and another slightly larger than 2.2 µm (see Fig. S1). *Synechococcus* was isolated from the nanoeukaryotes by its pigment characteristics – both subgroups of *Synechococcus* had high PE relative to APC content (Barlow et al., 1985; Marie et al., 1997), whereas nanoeukaryotes had high APC and PE.

Since no direct measurements of NH_4^+ regeneration (i.e., heterotrophy) were made in this study, potential heterotrophic activity is evaluated from the abundance of heterotrophic cells determined via flow cytometry and the ratio of bulk POC to PON concentrations (POC:PON). The availability of organic matter to heterotrophs is estimated from the abundance of detritus and the ratio of POC-to-chl-a concentrations (POC:chl-a; Holm-Hansen et al., 1989).

The correlations among latitude, N concentrations, inorganic carbon and N uptake rates, and NH_4^+ oxidation rates were investigated at the 5% significance level using the Pearson correlation coefficient and the R packages, stats (R Core Team, 2020) and corrplot (Wei & Simko, 2017).

4. Results

4.1 Hydrography

Sea surface temperature (SST) decreased from Cape Town (~34°S) to the edge of the MIZ (61.7°S) by ~17 °C (Fig. 1). During leg N, fairly deep MLDs were observed (124-212 m), similar to June and July climatological MLDs compiled from Argo float data for this region (Dong et al., 2008). While the focus of this study is the surface (i.e., upper ~10 m), we describe the hydrography of the mixed layer here to demonstrate that sampling took place under conditions typical of winter, with the deep MLDs evincing ongoing wintertime mixing and associated nutrient recharge. Where not specified, the trends discussed below refer to the surface data only. For each parameter, the average ± 1 standard deviation (SD) calculated for each Southern Ocean zone is reported in Table 1.

4.2 Macronutrient concentrations

https://doi.org/10.5194/bg-2021-149
Preprint. Discussion started: 10 June 2021

363 The surface and mixed-layer concentrations of NH_4^+ ranged from below detection to 0.70 µM
364 along legs S and N (Fig. 2a and b). The concentrations were higher in the PFZ, OAZ, and PAZ
365 (0.42 ± 0.01 µM, 0.52 ± 0.01 µM, and 0.58 ± 0.01 µM, respectively) than in the Subtropical
366 Zone (STZ) and SAZ (0.08 ± 0.03 µM and 0.06 ± 0.01 µM, respectively), with a sharp gradient
367 observed in the PFZ, just south of the SAF. South of the SAF, high NH_4^+ concentrations
368 persisted near-homogeneously throughout the mixed layer, ranging from 0.65 ± 0.01 µM at
369 station 58.5°S to 0.27 ± 0.01 µM at station 48.0°S, with concentrations that were below
370 detection north of the SAF (Fig. 2b). Beneath the mixed layer, the NH_4^+ concentration
371 decreased rapidly at all stations to values below detection by 200 m.

372 The concentrations of PO_4^{3-} and NO_3^- increased southwards from <1 µM and <10 µM in the
373 STZ to >1.5 µM and >20 µM in the PFZ, OAZ, and PAZ (Fig. S2a and 2c), with the sharpest
374 gradients occurring near the SAF. The concentrations of $Si(OH)_4$ increased rapidly across the
375 PF, from an average of 3.2 ± 1.1 µM between 35.0°S and 48.0°S to 45.6 ± 0.6 µM between
376 52.1°S and 58.9°S (Fig. S2c). The NO_2^- concentrations were consistently low across the
377 transect (0.16 ± 0.02 µM; Fig. S2b), as were the concentrations of urea (0.20 ± 0.04 µM),
378 although slightly lower urea concentrations were observed in the SAZ than in the other zones.

379 4.3 Chlorophyll-a, POC and PON

380 The highest bulk (i.e., >0.3 µm) [chl-a] was observed near the South African continental shelf,
381 decreasing across the STF and remaining low thereafter (Fig. 3a), consistent with previous
382 autumn and winter studies (Froneman et al., 1999; Philibert et al., 2015; Scharek et al., 1994).
383 The proportion of chl-a in the >2.7 µm size class (hereafter, "nano+" size class) varied across
384 the region but was >50% at all stations, with higher (>80%) contributions near the fronts and at
385 many OAZ and PAZ stations (Fig. 3b). The nano+ contribution was ≤60% at only five stations
386 (three in the SAZ, two in the OAZ).

387 The concentrations of bulk POC and PON were highest north of the STF and slightly higher in
388 the OAZ than in the SAZ and PFZ (Fig. S3a and b). The contribution of the nano+ size fraction
389 to POC and PON across the transect was 80.6 ± 31.8% and 69.8 ± 50.3%, respectively (Fig.
390 S3c and d). The ratio of bulk POC:chl-a (weight:weight) was on average low in the STZ, SAZ,
391 and PFZ, and reached a maximum in the OAZ (Fig. 4a). Contrastingly, the ratio of POC:PON
392 (mol:mol) appeared to decrease southwards, although there was no significant difference
393 among zones (p-value > 0.05) (Fig. 4b). The δ^{15}N-PON also decreased southwards from the
394 STZ and SAZ to the PFZ and OAZ (Fig. 4c). Despite considerable differences among zones,
395 the δ^{15}N-PON was relatively homogenous within each zone.

396 4.4 Rates of net primary production, nitrogen uptake, and ammonium oxidation

397 The surface rates of bulk NPP were high in the STZ, and two- to six-fold higher in the SAZ and
398 PFZ than has been reported previously for the Atlantic sector in winter (Mdutyana et al., 2020;
399 Froneman et al., 1999) (Fig. 5a). By contrast, NPP was low in the OAZ, consistent with
400 previous measurements (Kottmeier & Sullivan, 1987; Mdutyana et al., 2020). The relative
401 contribution of the small size class (0.3-2.7 µm) generally increased southwards, from 14.6% at
402 37.0°S to 75.6% at 53.5°S, before decreasing to <20.0% at ~55.5°S near the SACCF.

https://doi.org/10.5194/bg-2021-149
Preprint. Discussion started: 10 June 2021

403 The bulk NH_4^+ uptake rates (ρNH_4^+) generally increased southwards from the STZ to the SAZ
404 and PFZ, and then decreased across the OAZ to reach a minimum at the southernmost station
405 (58.5°S; 3.0 ± 0.8 nM day^{-1}) (Fig. 5b). In the nano+ size fraction, ρNH_4^+ changed little
406 latitudinally, although it was slightly lower in the PFZ than in the other zones. The contribution
407 of nanoplankton to ρNH_4^+ ranged from 32.8% in the PFZ to 71.9% in the STZ. The bulk NO_3^-
408 uptake rates (ρNO_3^-) were also low in the STZ, while the highest ρNO_3^- was measured in the
409 SAZ before decreasing southwards. ρNO_3^- in the nano+ size class followed the same trend as
410 total community ρNO_3^-, with the nanoplankton accounting for 71.5 ± 0.3% of bulk ρNO_3^- on
411 average. The rates of bulk urea uptake (ρUrea) were highest in the STZ, with the SAZ and the
412 PFZ hosting similar rates, and the lowest rates were measured in the OAZ. ρUrea for the nano+
413 size class followed a similar trend to bulk ρUrea, and nanoplankton accounted for 51.8% of
414 ρUrea in the SAZ to 100% in the PAZ. The uptake rates of the different N forms were not
415 significantly correlated with one another or with the ambient N concentrations (Fig. S4).

416 Surface ammonium oxidation rates ($NH_4^+{}_{ox}$) increased southwards, with higher $NH_4^+{}_{ox}$ in the
417 OAZ and PAZ than in the STZ, SAZ, and PFZ (Fig. 5c). Generally, $NH_4^+{}_{ox}$ was comparable to
418 previous wintertime measurements from the surface of the open Southern Ocean (Bianchi et al.,
419 1997; Mdutyana et al., 2020), and also similar to summertime rates measured deeper in the
420 mixed layer in the Ross and Scotia Seas (Tolar et al., 2016). $NH_4^+{}_{ox}$ was not correlated with the
421 ambient NH_4^+ concentration (Fig. S4).

422 4.5 Plankton community composition

423 The abundance of microplankton, analysed at 16 stations on leg S, was generally low, with the
424 highest cell counts at stations 37.2°S and 41.3°S in the STZ and no cells counted at 38.1°S
425 (STZ) and 55.5°S (OAZ) (Fig. 6a). Total microplankton abundance was on average higher in
426 the STZ than in the SAZ, PFZ, and OAZ. The greatest diversity of microplankton groups was
427 observed at 41.3°S near the AF and at 50.0°S near the PF. The observation of enhanced
428 plankton diversity and abundance near the fronts, particularly the PF, is consistent with
429 previous studies showing higher biomass and variability in phytoplankton communities
430 associated with these features (Hense et al., 2000; Kopczynska et al., 2007; Moore & Abbott,
431 2000).

432 Centric diatoms (including *Planktoniella*, *Coscinodiscus*, and *Thalassiosira* species) were
433 detected only at 58.9°S (3 cells mL^{-1}), the southernmost station. Pennate diatoms (including
434 *Pseudo-nitzschia*, *Pleurosigma*, and *Navicula* species) were more abundant in the STZ, PFZ,
435 and OAZ, with negligible abundances observed in the SAZ. Higher pennate diatom abundances
436 occurred near the PF (7 cells mL^{-1}), as has been observed in summer (e.g., Bracher et al.,
437 1999). Dinoflagellates were identified at every station except 38.1°S and were most abundant
438 in the STZ and PFZ. At all but three stations, small (<15 µm) dinoflagellates were the most
439 abundant group, although the larger *Protoperidinium* dinoflagellate species (mainly
440 heterotrophic; Jeong & Latz, 1994) were almost as abundant in the PFZ and at 54.0°S. The
441 abundance of microzooplankton (ciliates only, 20-200 µm) was highest across the STZ, and
442 microzooplankton were also identified in the PFZ at 46.1°S (3 cells mL^{-1}) and 48.9°S (3 cells
443 mL^{-1}) and in the OAZ at 50.0°S (1 cells mL^{-1}) and 54.0°S (4 cells mL^{-1}). All other stations
444 were characterized by negligible (<1 cells mL^{-1}) microzooplankton abundances.

https://doi.org/10.5194/bg-2021-149
Preprint. Discussion started: 10 June 2021

Nano- and picoeukaryotes, *Synechococcus*, and small heterotrophs (collectively, "small cells") sampled at 13 stations along leg S were roughly 10^3-times more abundant than the microplankton (Fig. 6b). Notwithstanding a lack of data from the STZ, the highest small cell abundances occurred in the SAZ near the SAF. Across the transect, picoeukaryotes were generally more abundant than all other phytoplankton groups (average picoeukaryote contribution to total small cells of 12-54%; nanoeukaryotes of 7-39%; *Synechococcus* of 15-42%). A similar trend was observed previously for the Southern Ocean in spring (Detmer & Bathmann, 1997) and late summer (Fiala et al., 1998), in contrast to mid-summer observations showing nanoplankton dominance (e.g., Ishikawa et al., 2002; Weber & El-Sayed, 1987). Additionally, picoeukaryotes were two- to three orders of magnitude more abundant in the SAZ and PFZ than in the OAZ. Nanoeukaryotes dominated small cell abundances near the PF at 50.0°S (39%) and in the southern OAZ at 55.5°S (36%), while *Synechococcus* dominated at 42.7°S and 54.0°S (42% and 33%, respectively). Nanoeukaryote abundance was higher in the SAZ than in the PFZ and OAZ, as was the abundance of *Synechococcus*.

The relative contribution of heterotrophs to total small cells varied considerably (10-62%), reaching a maximum south of the PF at 53.0°S and 57.8°S (62% and 50%; Fig. 7a). Heterotroph abundance followed a similar pattern to that of the nanoeukaryotes, with higher abundances in the SAZ than in the PFZ and OAZ. The food source available to heterotrophs, represented by the small detrital particles, was highest near the southern edge of the SAF. More generally, detrital particles were more abundant in the PFZ than in the SAZ and OAZ. The relative contributions of detrital, photosynthetic, and heterotrophic particles are shown in Fig. S5.

5. Discussion

5.1 Drivers of NH_4^+ cycling in the surface layer of the Southern Ocean

Previous work has suggested that NH_4^+ accumulates in the Southern Ocean mixed layer following the late summer increase in zooplankton abundance and heterotrophic activity, then decreases into autumn as heterotrophic activity subsides, to be depleted by winter due to advective processes and consumption (Koike et al., 1986; Serebrennikova & Fanning, 2004). However, our data show that NH_4^+ concentrations are elevated in the Southern Ocean mixed layer in winter, particularly south of the SAF (Fig. 2). Similarly elevated winter surface-layer NH_4^+ has been observed previously in both the Atlantic and Indian sectors, with concentrations typically increasing towards the south (Philibert et al., 2015; Mdutyana et al., 2020; Bianchi et al., 1997). Numerous overlapping processes are likely involved in setting the ambient NH_4^+ concentrations, as summarized in Fig. 8. In this study, we directly measured the rates of NH_4^+ uptake by different size fractions of the winter plankton community, as well as the rates of NH_4^+ oxidation. We infer the contribution of heterotrophic bacteria and microzooplankton to NH_4^+ production from cell count data and the abundance of small heterotrophs relative to phytoplankton and detritus. For the NH_4^+ cycle processes in Fig. 8 that are not quantified or inferred here – microzooplankton grazing, atmospheric NH_4^+ deposition, NH_3 air-sea exchange, sea-ice melt, and dissolved organic nitrogen (DON) conversion to NH_4^+ –, we consider their potential role in Southern Ocean NH_4^+ cycling based on findings reported in the literature.

https://doi.org/10.5194/bg-2021-149
Preprint. Discussion started: 10 June 2021

The high NH_4^+ concentrations observed in the winter PFZ and AZ (OAZ + PAZ) may result from net NH_4^+ accumulation during late summer, autumn and/or winter. The persistence of high NH_4^+ concentrations that are near-homogeneously distributed throughout the mixed layer suggests a residence time for the winter NH_4^+ reservoir in excess of the time-scale for upper-ocean mixing. One implication of this suggestion is that the wintertime NH_4^+ pool likely reflects processes that occurred earlier in the season, as well as those that are ongoing. We posit that the elevated NH_4^+ concentrations in the PFZ and AZ may result from higher wintertime rates of NH_4^+ production than consumption and/or from the gradual but incomplete depletion in winter of NH_4^+ produced mainly in late summer and autumn. We evaluate both possibilities throughout the discussion below.

5.1.1 Ammonium consumption

Ammonium uptake – Microbial growth is limited in the winter Southern Ocean (Arrigo et al., 2008; Smith Jr et al., 2000, Takao et al., 2012), resulting in low cell abundances and nutrient uptake rates (Church et al., 2003; Iida & Odate, 2014; Mdutyana et al., 2020). While the concentrations of chl-a and rates of NPP were low across our transect, they were not negligible (Fig. 3a and 5a), consistent with previous reports for this season (Mordy et al., 1995; Pomeroy & Wiebe, 2001). Southern Ocean phytoplankton are adapted to survive suboptimal conditions; for example, numerous species achieve their maximum growth rates at temperatures that are considerably lower than the optimal growth temperatures of temperate and tropical species (2-9 °C versus 10-30 °C and 15-35 °C, respectively), with sharp declines in growth rates observed for temperatures outside this range (Boyd et al., 2013; Coello-Camba & Agusti, 2017; Fiala & Oriol, 1990). In addition, ice-free Southern Ocean waters typically extend to <60°S in the east Atlantic and west Indian sectors in winter, so that although irradiance levels may not be optimal for phytoplankton growth, there is always some light available for photosynthesis. The hostile conditions of the open winter Southern Ocean do not, therefore, prevent ecosystem functioning (Pomeroy & Wiebe, 2001), although the microbial dynamics and associated biogeochemical processes differ from those occurring in summer (Smart et al., 2015; Mdutyana et al., 2020).

We measured fairly low NH_4^+ uptake rates in surface waters (3.0-13.2 nM day^{-1}; Fig. 5b) compared to previous wintertime observations (ranging from 32-66 nM day^{-1}; Cota et al., 1992; Mdutyana et al., 2020; Philibert et al., 2015). Such low rates, if generally representative of winter, would limit mixed-layer NH_4^+ drawdown, especially south of the PF where ρNH_4^+ was particularly low. Recycled N (NH_4^+ + urea) nonetheless accounted for most of the N consumed, including in the AZ (Fig. 5b).

The δ^{15}N-PON data (Fig. 4c) suggest that this elevated reliance on recycled N persisted from the late summer. In theory, PON generated in early- through mid-summer from the consumption of upwelled NO_3^- (δ^{15}N-NO_3^- of 5.2‰ in the AZ and 6.2‰ in the SAZ; Smart et al., 2015; Fripiat et al., 2019) will have a δ^{15}N of ~0‰ in the AZ and 1-2‰ in the SAZ given the isotope effect of NO_3^- assimilation and the degree of seasonal NO_3^- drawdown (Sigman et al., 1999; Granger et al., 2004; 2010). Such δ^{15}N-PON values have indeed been observed in early- and mid-summer (Lourey et al. 2003; Smart et al. 2020; Soares et al., 2015). By late summer, δ^{15}N-PON declines to -5 to -1‰, with the lowest values occurring in the AZ (Lourey et al. 2003; Smart et al. 2020; Trull et al., 2008). Since the δ^{15}N of recycled N is expected to be

https://doi.org/10.5194/bg-2021-149
Preprint. Discussion started: 10 June 2021

low (<0‰; Checkley & Miller, 1989, Macko et al., 1986), the early-to-late summer decline in δ^{15}N-PON implicates a switch from dominantly NO_3^-- to dominantly recycled N-supported phytoplankton growth (Lourey et al., 2003). For the SAZ, the subsequent late summer-to-winter rise in δ^{15}N-PON (i.e., from ~ -1‰ to 1-2.5‰; Fig. 4c) has previously been attributed to PON decomposition by heterotrophic bacteria (Smart et al., 2020), during which ^{14}N-NH_4^+ is preferentially remineralized, leaving the remaining PON enriched in ^{15}N (Möbius, 2013). That NH_4^+ concentrations are not elevated in the SAZ mixed layer in winter (Fig 2b.) indicates that the remineralized NH_4^+ is rapidly re-assimilated by phytoplankton and/or oxidized to NO_2^- in this zone. In the AZ, the δ^{15}N-PON of -3 to -1‰ that we observe in winter surface waters requires the sustained consumption of low-δ^{15}N N (i.e., recycled NH_4^+ and urea) to offset a remineralization-driven δ^{15}N rise similar to that of the SAZ. We conclude that Southern Ocean phytoplankton dominantly consume regenerated N from late summer until at least July (albeit at low rates in winter), particularly south of the PF.

The fact that the NH_4^+ concentration was high in the winter mixed layer despite NH_4^+ being the preferred phytoplankton N source in late summer through winter implies that low rates of NH_4^+ uptake contributed to the accumulation of this N form. Multiple factors may cause low rates of photoautotrophic NH_4^+ uptake, including deplete NH_4^+ and micronutrient concentrations, light limitation, and low temperatures. North of the SAF, NH_4^+ concentrations below detection likely limited ρNH_4^+, as evidenced by the fact that in a series of experiments conducted on the same cruise, ρNH_4^+ increased with the addition of NH_4^+ at these stations (Mdutyana, 2021). By contrast, south of the SAF, NH_4^+ concentrations were similar to or higher than the half-saturation constant (K_m) derived for NH_4^+ uptake in the winter Southern Ocean (0.2 to 0.4 µM; Mdutyana, 2021), suggesting that something other than NH_4^+ availability was limiting to phytoplankton at these latitudes.

Iron is not directly involved in NH_4^+ assimilation but is required for electron transport during photosynthesis and respiration (Raven, 1988). While iron limitation is widespread across the Southern Ocean (Janssen et al., 2020; Pausch et al., 2019; Viljoen et al., 2019), iron availability appears to be higher in winter than during other seasons (Mtshali et al., 2019; Tagliabue et al., 2014) due to enhanced mixing, storms, and increased aeolian deposition (Coale et al., 2005; Honjo et al., 2000; Sedwick et al., 2008). The fact that ρNO_3^- and ρNH_4^+ were generally similar across the transect (Fig. 5b) argues against a dominant role for iron in controlling ρNH_4^+ since NO_3^- assimilation has a far higher iron requirement than NH_4^+ consumption (Morel et al., 1991).

In contrast to NH_4^+ and iron availability, light limitation is exacerbated in winter due to low insolation, increased cloud-cover, and mixed layers that can be hundreds of meters deeper than the euphotic zone (Brightman & Smith Jr., 1989; Buongiorno Nardelli et al., 2017; Sallée et al., 2010). Light is thus often considered the dominant constraint on Southern Ocean primary productivity in this season (Thomalla et al., 2011; Llort et al., 2019; Wadley et al., 2014). However, since NH_4^+ consumption by phytoplankton is fairly energetically inexpensive (Dortch, 1990), it should occur even under low light (recognizing that light remains critical for coincident CO_2 fixation). Heterotrophic bacteria can also consume NH_4^+ (Kirchman, 1994), including in the dark since they derive energy from organic carbon oxidation rather than light.

https://doi.org/10.5194/bg-2021-149
Preprint. Discussion started: 10 June 2021

571 At an ecosystem level, therefore, NH_4^+ consumption may not be primarily limited by light,
572 although this parameter clearly strongly controls the rate of NPP (Fig. 5a).

573 Previous observations suggest that temperature influences NH_4^+ uptake, especially in winter
574 (Glibert, 1982; Reay et al., 2001). The negative effect of temperature appears to be enhanced
575 under high-nutrient and low-light conditions, at least in the case of phytoplankton growth rates
576 (Baird et al., 2001). Additionally, Southern Ocean phytoplankton may be psychrotolerant and
577 not psychrophilic, which means that while they can function at *in situ* wintertime temperatures,
578 their optimal temperatures for growth and photosynthesis are higher (Reay et al., 2001; Smith
579 Jr & Harrison, 1991; Tilzer et al., 1986). Experiments conducted coincident with our sampling
580 showed that the maximum rate of NH_4^+ uptake (V_{max}) achievable by the *in situ* community was
581 strongly negatively correlated with temperature and latitude (Mdutyana, 2021), with the latter
582 parameter indicative of the combined role of light, temperature, and possibly iron, the
583 concentration of which appears to increase from the SAZ to the AZ (Tagliabue et al., 2012).
584 We conclude that these three drivers, along with NH_4^+ availability north of the SAF, all play a
585 role in controlling photoautotrophic NH_4^+ uptake in the winter Southern Ocean, with complex
586 interactions among them that are difficult to disentangle.

587 In addition to physical and chemical limitations, microbial preference for other N species may
588 impact the depletion of the NH_4^+ pool. For example, the preferential uptake of urea and other
589 DON species by some organisms (e.g., cyano- or heterotrophic bacteria) could dampen total
590 NH_4^+ uptake rates. While large contributions of urea to total N uptake have previously been
591 observed in the Southern Ocean in summer and autumn (predominantly in the SAZ; Joubert et
592 al., 2011; Thomalla et al., 2011), we measured fairly low ρUrea (Fig. 5b), which is perhaps
593 unsurprising given the low ambient urea concentrations (Table 1). The exceptions were stations
594 37°S and 43.0°S where ρUrea was higher than ρNH_4^+, coincident with very low ambient NH_4^+
595 (0.10 µM and below detection) and relatively high urea concentrations (0.36 µM and 0.15 µM).

596 Community composition can also alter the N uptake regime. Smaller phytoplankton, such as
597 the numerically-dominant nano- and picoeukaryotes, are more likely to consume NH_4^+ and urea
598 than NO_3^- (Koike et al., 1986; Lee et al., 2012, 2013), especially in the Southern Ocean where
599 NO_3^- assimilation is severely limited by iron and light availability (Sunda & Huntsman, 1997).
600 Across our transect, the sum of NH_4^+ and urea uptake (i.e., reduced N uptake) exceeded NO_3^-
601 uptake for both the total phytoplankton community (transect average of 12.0 ± 0.9 nM day^{-1} for
602 reduced N versus 5.8 ± 1.0 nM day^{-1} for NO_3^-; f-ratio of 0.36) and the 0.3-2.7 µm size fraction
603 (5.0 ± 1.2 nM day^{-1} versus 1.9 ± 1.2 nM day^{-1}; f-ratio of 0.27 (Fig. 5b). That said, the NO_3^-
604 uptake rates were not negligible, including in the 0.3-2.7 µm size fraction. In the PFZ and AZ,
605 NO_3^- uptake by the 0.3-2.7 µm size fraction was more strongly correlated with the abundance
606 of picoeukaryotes than *Synechococcus* (r = 0.75 and 0.03, respectively), consistent with
607 observations of dominant reliance on NO_3^- by picoeukaryotes and NH_4^+ by *Synechococcus* in
608 other ocean regions (Casey et al., 2009; Fawcett et al., 2011, 2014; Treibergs et al., 2014;
609 Painter et al., 2014). Nonetheless, *Synechococcus* can consume all N forms (Capone et al., 2008
610 and references therein) and has evolved strategies to conserve iron by using other trace metals
611 in some enzymes (Palenik et al., 2003). Thus, *Synechococcus* may be adapted to consume NO_3^-
612 in the Southern Ocean when reduced N concentrations are near depletion (e.g., north of the
613 SAF in winter), but are likely to consume NH_4^+ as long as it is available, as implied by their

https://doi.org/10.5194/bg-2021-149
Preprint. Discussion started: 10 June 2021

strong correlation with NH_4^+ concentration south of the SAF (r = 0.65). In the nano+ size class, NO_3^- uptake was likely driven in the SAZ by dinoflagellates and some nanoeukaryotes, and in the PFZ and AZ by diatoms, which remain active in these zones in winter (Weir et al., 2020). By contrast, nanoeukaryotes, which have a higher per-cell nutrient requirement than the equally-abundant picoeukaryotes, may have dominated NH_4^+ uptake in the PFZ and AZ given that higher nanoeukaryote abundances corresponded with lower NH_4^+ concentrations at a number of stations (e.g., stations 50.0°S, 51.1°S, and 55.5°S; Fig. 6b).

The low abundances of diatoms and dinoflagellates and absence of coccolithophores (Fig. 6a) across our transect is expected given the limitations imposed on nutrient uptake and CO_2 fixation by winter Southern Ocean conditions. The lower surface area-to-volume ratio of larger cells means that they rapidly experience diffusion-limitation of NH_4^+ and micronutrient uptake and are more susceptible to light limitation (Finkel et al., 2004), resulting in their being outcompeted by smaller species for essential resources (Franck et al., 2005; Cavender-Bares et al., 1999). The near-absence of centric diatoms is also best explained thus, particularly given their low surface area-to-volume ratio compared to pennate species (Kobayashi & Takahashi, 2002) that are more likely to consume NH_4^+ (Semeneh et al., 1998) and were more abundant. That said, we did not observe a clear relationship between pennate diatom abundance and NH_4^+ concentration, except proximate to the PF (stations 47.9°S, 48.9°S, and 50.0°S) where higher pennate abundance was associated with lower NH_4^+. Diatom success in winter may also be limited by enhanced mixing, as this group is generally adapted for stratified waters (Kopczynska et al., 2007).

In sum, NH_4^+ uptake rates were low across our transect but not negligible, indicating that phytoplankton activity in winter, which is dominated by smaller species, represents a sink for NH_4^+. Hostile Southern Ocean conditions imposed limitations on NH_4^+ uptake that varied with latitude, with NH_4^+ concentrations controlling ρNH_4^+ north of the SAF, while light and temperature were important south of the SAF, with a possible supporting role for iron. Additionally, *Synechococcus,* nanoeukaryotes, and pennate diatoms likely dominated NH_4^+ consumption, consistent with previous observations from the Southern Ocean and elsewhere (Klawonn et al., 2019; Semeneh et al., 1998).

Ammonium oxidation – Nitrification removes more mixed-layer NH_4^+ than phytoplankton consumption south of the PF, with NH_4^+ oxidation rates that were two- to five-times the co-occurring NH_4^+ uptake rates (Fig. 5c). The comparative success of NH_4^+ oxidisers may be due to decreased competition with phytoplankton for NH_4^+ in winter, augmented by decreased photoinhibition (Wan et al., 2018; Lu et al., 2020) and elevated NH_4^+ availability (Baer et al., 2014; Mdutyana et al., 2020; Mdutyana, 2021). One implication of the dominance of NH_4^+ oxidation is that in addition to the limitations on phytoplankton NH_4^+ uptake discussed above, low phytoplankton success in the AZ may also result from nitrifiers outcompeting phytoplankton under conditions of low incident light and enhanced mixing for scarce resources (e.g., trace elements required for enzyme functioning, such as iron and copper; Shafiee et al., 2019; Maldonado et al., 2006; Amin et al., 2013).

Although NH_4^+ oxidisers appear to be truly psychrophilic given the southward increase in NH_4^+ oxidation rates, the effect of temperature is difficult to disentangle in an environment with

https://doi.org/10.5194/bg-2021-149
Preprint. Discussion started: 10 June 2021

multiple overlapping drivers. While several studies have reported a minimal effect of temperature on NH_4^+ oxidation rates (Bianchi et al., 1997; Baer et al., 2014; Horak et al., 2013; Mdutyana et al., in review), nitrifiers in the winter Southern Ocean may yet be living at suboptimal temperatures (Jones et al., 1988). Indeed, a relative inefficiency of NH_4^+ oxidation at low temperatures could be inferred from the general southward increase in the ratio of NH_4^+ to NO_2^- concentration (NH_4^+:NO_2^-; Fig. S6). This trend is unexpected given the lower affinity of nitrite oxidizing bacteria for NO_2^- compared to that of ammonia oxidisers for NH_4^+, which should result in an accumulation of NO_2^- relative to NH_4^+ (Pachiadaki et al., 2017; Zakem et al., 2018; Zhang et al., 2020). However, other factors such as mixing and increased predation and viral lysis can also affect NH_4^+:NO_2^-, and the dynamics of NH_4^+ are less predictable in space and time than those of NO_2^- because of their different residence times (Zakem et al., 2018).

The K_m derived for NH_4^+ oxidation in the winter Southern Ocean has recently been reported to be low (0.03 to 0.14 µM), with ammonia oxidizers observed to become saturated at ambient NH_4^+ concentrations of ~0.1-0.2 µM (Mdutyana, 2021). This means that south of the SAF in winter 2017, ammonia oxidizers were not substrate limited (further implied by the lack of correlation between $NH_4^+{}_{ox}$ and NH_4^+ concentration; Fig. S4), which raises the question of why NH_4^+ oxidation did not occur at higher rates. The answer may involve temperature, in that psychrophilic organisms can be less responsive to high substrate concentrations at low temperatures (Baer et al., 2014). Another possibility is that NH_4^+ oxidation was iron-limited (Shiozaki et al., 2016; Mdutyana, 2021), with a recent culture study revealing the surprisingly low affinity for iron of the globally-abundant ammonia oxidiser, *Nitrosopumilus maritimus* (Shafiee et al., 2019). In any case, NH_4^+ oxidisers were moderately successful across the surface Southern Ocean in winter, with low light, reduced competition with phytoplankton, and substrate repletion likely explaining the elevated NH_4^+ oxidation rates south of the PF compared to the stations to the north.

5.1.2 Ammonium production and other inputs

NH_4^+ production, although not measured directly in this study, must be sustained during the winter to retain an NH_4^+ pool that is high in concentration relative to the early summer. With low or no NH_4^+ production in the autumn and winter, the NH_4^+ pool south of the SAF would be depleted in 10 to 38 days (median of 21 days) given the consumption rate ($\rho NH_4^+ + NH_4^+{}_{ox}$) and NH_4^+ concentration measured at each station (Text S2). Heterotrophic NH_4^+ production must, therefore, be ongoing in winter despite the limited production of PON substrate.

Heterotrophic activity by bacteria – Heterotrophic bacteria may contribute significantly to NH_4^+ accumulation via ammonification of organic N (Hewes et al., 1985; Koike et al., 1986; Treguer & Jacques, 1992), including in winter (Rembauville et al., 2017). However, since these bacteria are likely more active in late summer and autumn when both temperature and the supply of fresh PON are high (Becquevort et al., 2000; Dennet et al., 2001), we expect that the winter NH_4^+ pool includes residual NH_4^+ produced towards the end of the growing season. At the time of our sampling, heterotrophic abundances were ten-fold lower to two-fold higher than total pico- and nanophytoplankton abundances (Fig. 7a). Higher ratios of heterotrophic-to-photosynthetic cells occurred at stations with higher NH_4^+ concentrations (e.g., stations 48.9°S, 53.0°S, 54.0°S and 57.8°S), suggesting a role for the short-term balance between NH_4^+

https://doi.org/10.5194/bg-2021-149
Preprint. Discussion started: 10 June 2021

698 production and consumption in controlling the ambient NH_4^+ concentration in winter. The
699 heterotrophic bacteria were likely consuming detritus (as opposed to living cells), with the
700 relative availability of detrital substrate evident from the high detrital particle counts (Fig. 7b)
701 and the persistently high POC:chl-a ratios, particularly south of the PF (Fig. 4a; Holm-Hansen
702 et al., 1989). Additionally, a southward increase in heterotrophic biomass (which has a C:N
703 ratio typically ≤5:1) can be inferred from the southward decline in POC:PON (Fig. 4b; Frigstad
704 et al., 2011; del Giorgio & Cole, 1998), although this could also be due to iron and light
705 limitation of CO_2 fixation (Mongin et al., 2006; Talmy et al., 2016). Active remineralization of
706 detritus south of the SAF is further implicated by lower ratios of detrital-to-heterotrophic
707 particles coincident with higher NH_4^+ concentrations (Fig. 7b). Finally, the specific uptake rate
708 of NO_3^- + NH_4^+ + urea (i.e., V_{Ntot}) exceeded that of CO_2 fixation (V_C) at some AZ stations (Fig.
709 S7). Similar observations in the winter Southern Ocean have been interpreted as indicating the
710 consumption of reduced N by heterotrophic bacteria (thus evincing their activity), which occurs
711 in the absence of CO_2 fixation, thereby decoupling V_C and V_{Ntot} (Text S2; Mdutyana et al.,
712 2020).

713 Despite the indirect evidence for an active heterotrophic bacterial population at the time of
714 sampling, it is possible that heterotrophic activity was also limited in the wintertime Southern
715 Ocean, in part because PON concentrations are generally low in this season (Pomeroy &
716 Wiebe, 2001; Smart et al., 2020). That said, bacteria may be more efficient at lower
717 temperatures than phyto- and zooplankton given their similar metabolic rates in temperate and
718 polar waters (Pomeroy & Wiebe, 2001 and references therein). Additionally, bacteria may be
719 less vulnerable to resource limitation because of their small size. Only slight differences in Q_{10}
720 values (i.e., the proportional increase in growth rate with a 10 °C rise in temperature) between
721 phytoplankton and heterotrophs are required for heterotrophic NH_4^+ production to exceed
722 phytoplankton NH_4^+ uptake (Koike et al., 1986). Nonetheless, it is highly unlikely that the
723 surface NH_4^+ pool measured in winter derived solely from wintertime bacterial production
724 given that yet higher NH_4^+ concentrations have been observed in late summer/autumn
725 (Becquevort et al., 2000; Dennett et al., 2001); this is discussed further in section 5.2 below.

726 *Heterotrophic activity by zooplankton* – The microzooplankton enumerated in this study may
727 also contribute to NH_4^+ accumulation, although they are probably less important in winter than
728 heterotrophic bacteria given their low and variable abundances (Fig. 6a). At the PFZ and AZ
729 stations characterized by high ratios of heterotrophic-to-photosynthetic cells but relatively low
730 absolute heterotrophic bacterial abundances, the coincident elevated NH_4^+ concentrations could
731 be due to the higher microzooplankton abundances compared to other stations (e.g., station
732 54.0°S). In other words, elevated microzooplankton abundances may help to explain the high
733 NH_4^+ concentrations at stations where the abundance of small heterotrophs was relatively low.

734 Above, we have assumed that the pathways leading to NH_4^+ production are associated with
735 heterotrophy. However, there are other possible mechanisms of NH_4^+ generation that should be
736 considered.

737 *DON cycling* – NH_4^+ can be released by heterotrophic bacteria that directly consume DON
738 (e.g., urea) (Billen, 1983; Tupas & Koike, 1990), and possibly also by ammonia oxidisers that
739 convert DON to NH_4^+ intracellularly, through the equilibration between intra- and extracellular

https://doi.org/10.5194/bg-2021-149
Preprint. Discussion started: 10 June 2021

740 NH_4^+ pools (Kitzinger et al., 2019). DON can also be converted to NH_4^+ through
741 photodegradation by UV radiation (e.g., Aarnos et al., 2012). However, bacterial
742 decomposition of DON (rather than PON) to NH_4^+ is implicit in most estimates, qualitative and
743 quantitative, of heterotrophic bacterial remineralization. Additionally, the magnitude of cellular
744 NH_4^+ efflux by ammonia oxidisers is likely be extremely low given that they also require NH_4^+
745 to fix CO_2. Finally, the low light levels of the wintertime Southern Ocean mean that
746 photodegradation is unlikely to yield a significant NH_4^+ flux. We thus conclude that DON
747 conversion to NH_4^+, through any mechanism, is probably negligible.

748 *External inputs of ammonium* – High surface ocean NH_4^+ concentrations may theoretically
749 derive from external inputs of NH_4^+, such as from nitrogen fixation, NH_4^+ aerosol deposition, or
750 sea-ice melt. Nitrogen fixation should be negligible in the winter Southern Ocean due to the
751 extremely cold temperatures, low light and iron availability, and high NO_3^- concentrations
752 (Jiang et al., 2018; Knapp et al., 2012; Kustka et al., 2003). Similarly, NH_4^+ aerosols are
753 unlikely to be abundant over regions of the Southern Ocean remote from islands and coastal
754 Antarctica. Those that are present mainly originate from surface ocean NH_3 efflux; once re-
755 deposited, this NH_4^+ does not constitute a new input term to surface waters (Altieri et al., 2021).
756 Additionally, NH_4^+ aerosol concentrations are at a minimum in winter (Legrand et al., 1998; Xu
757 et al., 2019). NH_4^+ deposition to the surface Southern Ocean is thus likely minimal. Finally,
758 since our sampling took place before the sea-ice reached its northernmost extent (Cavalieri &
759 Parkinson, 2008), the dominant process would have been sea-ice formation rather than sea-ice
760 melt, the latter a source of NH_4^+ at times (Kattner et al., 2004; Zhou et al., 2014), although
761 probably not during our study. Additionally, we observed elevated NH_4^+ as far north as 46ºS,
762 which is ~1700 km beyond the reach of sea-ice melt.

763 5.2 Seasonal cycling of NH_4^+ in the Southern Ocean mixed layer south of the SAF

764 To contextualize our wintertime observations, we need to explore the seasonality of the NH_4^+
765 pool in the surface Southern Ocean, especially given that NH_4^+ production in late summer and
766 autumn almost certainly contributes to wintertime NH_4^+ accumulation. Surface NH_4^+
767 concentrations were measured during three additional cruises in the Atlantic sector (December
768 2018-March 2019, early- and late summer; July-August 2019, winter; October-November
769 2019, spring; Fig. 9a-e). During these cruises, underway samples were collected for analysis of
770 NH_4^+ concentrations every two hours between Cape Town and Antarctica (early- and late
771 summer) or the MIZ (winter and spring), and analysed as described in section 3.2.1 for winter
772 2017.

773 In early summer, the surface NH_4^+ concentrations were uniformly low across the transect
774 (average of 0.11 ± 0.09 µM; Fig. 9a) due to rapid consumption by phytoplankton, as has been
775 observed previously (Mdutyana et al., 2020; Savoye et al., 2004; Daly et al., 2001). South of
776 the SAF, NH_4^+ concentrations increased significantly as the growing season progressed,
777 reaching an average concentration of 0.81 ± 0.92 µM by late summer (Fig. 9b). This NH_4^+
778 increase can be explained by elevated heterotrophic activity following the spring/summer
779 phytoplankton bloom (Mengesha et al., 1998; Le Moigne et al., 2013), coupled with iron-
780 and/or silicate-limitation of phytoplankton (Hiscock et al., 2003; Sosik & Olson, 2002) and
781 enhanced grazing pressure (Becquevort et al., 2000). The NH_4^+ concentrations measured south

https://doi.org/10.5194/bg-2021-149
Preprint. Discussion started: 10 June 2021

of the SAF during the 2019 winter cruise (Fig. 9c) were similar to those observed in winter 2017 (0.48 ± 0.30 µM and 0.52 ± 0.11 µM, respectively), confirming that our 2017 observations are generally representative of the wintertime Southern Ocean. Additionally, the winter measurements indicate that mixed-layer NH_4^+ concentrations remain high between late summer and winter, consistent with sustained heterotrophic NH_4^+ production.

Our hypothesis for sustained late summer-to-winter heterotrophic activity is supported by calculations of the residence time of NH_4^+ south of the SAF (Text S3). Using the NH_4^+ concentrations and ρNH_4^+ measured in late summer 2019 (Deary, 2020), we calculate that the NH_4^+ pool would be depleted in 2 to 27 days (median of 5 days) without coincident NH_4^+ production. Indeed, given the average ρNH_4^+ south of the SAF in late summer (50.6 ± 24.0 nM/day), the net decline in NH_4^+ concentration of 0.33 ± 0.97 µM between late summer and winter (a roughly four-month period) requires an average NH_4^+ production rate of 52.9 ± 25.0 nM/day. This estimate is comparable to NH_4^+ remineralisation rates measured in the AZ near the Antarctic Peninsula in summer (the only measurements of NH_4^+ regeneration available for the Southern Ocean; average of 55 nM day^{-1}; Goeyens et al., 1991).

By the early spring, the NH_4^+ concentrations south of the SAF had declined to near or below the methodological detection limit (0.09 ± 0.08 µM; Fig. 9d), implicating increased photosynthetic activity following the alleviation of light-limitation that results in the consumption of nutrients introduced into surface waters in winter. We postulate that the residual NH_4^+ would have been consumed prior to significant NO_3^- drawdown because far less energy (i.e., light) is required for its assimilation (Dortch, 1990). NH_4^+ concentrations south of the SAF rose again by the late spring to an average value only slightly lower than that measured in winter (0.37 ± 0.69 µM; Fig. 9e). However, late-spring NH_4^+ concentrations were only elevated in the PFZ (range of 0.11 ± 0.01 to 4.39 ± 0.03 µM, average of 0.71 ± 1.04 µM), as has been observed previously (Bathmann et al., 1997), which we attribute to increased heterotrophic activity in response to elevated regional springtime phytoplankton growth driven by frontal upwelling (Becquevort et al., 2000; Mayzaud et al., 2002). Excluding the PFZ data yields a far lower late-spring average NH_4^+ concentration of 0.18 ± 0.14 µM, which we take as broadly representative of this season.

Using our high-resolution NH_4^+ concentration measurements, we propose a seasonal cycle for mixed-layer NH_4^+ south of the SAF (Fig. 9f). Our proposal is consistent with previous characterizations of the early summer-to-autumn evolution of Southern Ocean NH_4^+ concentrations (i.e., from below detection due to phytoplankton uptake to elevated due to net heterotrophic activity), but contradicts the hypothesis that NH_4^+ will subsequently decline due to persistent but low rates of photosynthesis that yield insufficient biomass to support late-summer heterotrophy, thus resulting in a coincident decrease in photosynthetic and heterotrophic activity (Koike et al., 1986; Serebrennikova & Fanning, 2004). Instead, our data evince a gradual decline in mixed-layer NH_4^+ concentrations from late summer through winter that we attribute to heterotrophic NH_4^+ production outpacing NH_4^+ consumption in late summer/autumn, with NH_4^+ regeneration then decreasing during winter to lower rates than the combination of phytoplankton NH_4^+ consumption and NH_4^+ oxidation. By late spring, NH_4^+ reaches concentrations similar to those observed in early summer as the improved growing conditions (i.e., elevated light and iron availability; Ellwood et al., 2008; Mtshali et al., 2019)

https://doi.org/10.5194/bg-2021-149
Preprint. Discussion started: 10 June 2021

allow phytoplankton to rapidly consume any NH_4^+ remaining at the end of winter and subsequently produced in spring. An exception to this scenario is elevated (and localized) NH_4^+ production near fronts, such as in late spring 2019, which likely resulted from biological activity supported by frontal upwelling of silicate- and iron-bearing Upper Circumpolar Deep Water (Prézelin et al., 2000).

5.3 Implications

Potential for ammonium inhibition of nitrate uptake – The low rates of NO_3^- uptake characteristic of winter Southern Ocean surface waters have been attributed to light, temperature, and micronutrient (especially iron) limitation of phytoplankton growth (Martin et al., 1990; Reay et al., 2001; Strzepek et al., 2019; Sunda & Huntsman, 1997). Wintertime NO_3^- uptake may be further inhibited by the high NH_4^+ concentrations (Goeyens et al., 1995; Philibert et al., 2015; Reay et al., 2001), as has been observed in other regions (Dortch, 1990; Flynn et al., 2018). Previous Southern Ocean studies have identified an inhibitory effect of NH_4^+ on NO_3^- uptake at NH_4^+ concentrations >1 µM (and occasionally between 0.5 µM and 1 µM; Cochlan, 1986; Cochlan et al., 2002; Kristiansen & Farbrot, 1991; Reay et al., 2001). Such concentrations were measured at a number of stations along our 2019 transects (Fig. 9b,c,e; and in 2017 if inhibition occurs at NH_4^+ concentrations of 0.5 µM; Fig. 1). If the seasonal accumulation of NH_4^+ inhibits NO_3^- drawdown, this amounts to an inefficiency in the biological pump. However, some culture studies report only a slight inhibition of NO_3^- uptake, even at high NH_4^+ concentrations (>>1 µM; Bagwell, 2009; Dortch, 1990 and references therein), while others have detected no influence of NH_4^+ on NO_3^- consumption (Rees et al., 1999), suggesting that this effect is not straightforward. In winter 2017, we observed little evidence of NH_4^+ inhibition of NO_3^- uptake – for example, the southward decrease in ρNO_3^- was not sharper than that of ρNH_4^+ despite the increase in NH_4^+ concentration, and we observed no relationship between NH_4^+ concentration and the proportion of NO_3^--to-total N uptake (i.e., the f-ratio, r = 0.28 including urea; n=7). We conclude that NH_4^+ inhibition of NO_3^- uptake is unlikely in open Southern Ocean surface waters, but may occur near fronts and/or the coasts of islands and Antarctica where NH_4^+ can accumulate to concentrations >>1 µM (Henley et al., 2017; Koike et al., 1986; Krell et al., 2005; Goeyens et al., 1995). In the case of coastal waters, the damping effect of NH_4^+ inhibition on the biological pump is only relevant if the NH_4^+ being consumed in lieu of NO_3^- derives from *in situ* regeneration rather than being supplied from land.

Palaeoceanographic proxies – NH_4^+ cycling in the Southern Ocean mixed layer may be important for palaeoceanographic proxies (Smart et al., 2020; Robinson et al., 2020), such as those that use the $\delta^{15}N$ of organic matter preserved in fossil foraminifer or diatom shells to infer the extent of upper ocean NO_3^- consumption in the past (and by extension, the role of Southern Ocean biology in determining atmospheric CO_2; e.g., Martínez-García et al., 2014; Studer et al., 2015). A recent ground-truthing study from the Southern Ocean showed that the $\delta^{15}N$ of foraminifer-bound organic N tracks the $\delta^{15}N$ of PON rather than NO_3^- (Smart et al., 2020), in contrast to results from the low-latitude ocean (Ren et al., 2012; Smart et al., 2015). Between summer and winter, the $\delta^{15}N$ of mixed-layer PON declines in the Southern Ocean (particularly in the AZ) due to enhanced mixed-layer NH_4^+ cycling (Fig. 4c; Lourey et al., 2003); this decrease will subsequently be reflected in the $\delta^{15}N$ of the foraminifera that feed on

https://doi.org/10.5194/bg-2021-149
Preprint. Discussion started: 10 June 2021

PON (Smart et al., 2020) and the late summer/autumn diatom communities that consume proportionally more NH_4^+ relative to NO_3^- than in spring and early summer (Studer et al., 2015; Kemeny et al., 2018). Thus, a decrease in the $\delta^{15}N$ of fossil foraminifera or diatoms could reflect enhanced NH_4^+ consumption by the upper ocean ecosystem rather than a change in the extent of NO_3^- drawdown, although this will depend on the degree to which surface conditions in the different seasons are communicated to the sediments (Smart et al., 2020). Further clarifying the seasonal mixed-layer NH_4^+ cycle in the Southern Ocean may thus aid interpretations of palaeoceanographic records.

Ocean ammonia emissions – The implications of NH_4^+ cycling extend beyond the upper ocean to the atmosphere. Ammonium aerosols that influence Earth's albedo through scattering and absorption of solar radiation and cloud formation (Tevlin & Murphy, 2019) are formed in the marine boundary layer from reactions of NH_3 gas with acidic species, usually sulfur derived from surface ocean dimethylsulfide emissions. The ocean is the largest natural source of NH_3 globally, however, the magnitude of the marine NH_3 source remains highly uncertain (Paulot et al., 2015). Surface ocean NH_4^+ concentrations play a central role in determining the sign and magnitude of the air-sea NH_3 flux, along with wind speed, surface ocean temperature, and pH. Therefore, the biogeochemical pathways that drive seasonality in surface ocean NH_4^+ concentrations are an important control on the remote Southern Ocean air-sea NH_3 flux, with implications for aerosol composition, cloud formation, and climate (Altieri et al., 2021).

6. Summary

This study, conducted in the Southern Ocean during the infrequently-sampled winter season, provides new insights into the internal cycling of N in the mixed layer of a globally-important region. We used measurements of NO_3^-, NH_4^+, and urea uptake, NH_4^+ oxidation rates, $\delta^{15}N$-PON, and the ratio of heterotrophic-to-photosynthetic cells to investigate NH_4^+ consumption, and the ratios of POC:chl-a and POC:PON, the relationship of V_{Ntot} to V_C, and measurements of plankton community composition to evaluate the potential for heterotrophic NH_4^+ production. We attribute the elevated NH_4^+ concentrations that persist in the winter mixed layer south of the SAF to sustained heterotrophic NH_4^+ production in excess of phytoplankton- and nitrifier-mediated NH_4^+ consumption, driven by temperature-, light-, and possibly iron-limitation of the NH_4^+ consumers. We further conclude that heterotrophic bacteria are the main NH_4^+ producers in winter and that the contributions of DON degradation, nitrogen fixation, aerosol deposition, and sea-ice melt to the Southern Ocean's mixed-layer NH_4^+ pool are negligible. Future measurements of heterotrophic NH_4^+ production rates are required to validate our conclusions, and higher spatial resolution sampling of community composition and N consumption rates may help to explain smaller-scale variability in NH_4^+ concentrations, particularly near the fronts.

From observations of surface NH_4^+ concentrations made between December 2018 and November 2019, we suggest that the high-concentration NH_4^+ pool cannot be generated solely during winter. Instead, we propose that NH_4^+ initially accumulates in late summer following the peak phytoplankton growing season, after which sustained heterotrophy throughout the autumn and winter prevents this NH_4^+ from being depleted until the early spring. The persistence of elevated NH_4^+ concentrations across the polar Southern Ocean between late summer and winter

https://doi.org/10.5194/bg-2021-149
Preprint. Discussion started: 10 June 2021

implies that the mixed layer is a biological source of CO_2 to the atmosphere for at least half the year, not only because NO_3^- drawdown is weak at this time (Arteaga et al., 2019; Johnson et al., 2017), but also because the ambient conditions allow for NH_4^+ accumulation. Additionally, high surface ocean NH_4^+ concentrations may alter components of the ocean-atmosphere NH_x cycle and may have implications for palaeoceanographic reconstructions based on N isotope measurements.

Acknowledgements

We acknowledge Captain Knowledge Bengu and the crew of the R/V *SA Agulhas II*, and Chief Scientists Hermann Luyt, Marcello Vichi, and Thomas Ryan-Keogh. We thank Tahlia Henry for CTD operations and CTD and SDS data processing. We are grateful to the students from the Cape Peninsula University of Technology for help with sample collection and analysis of chl-a samples. We thank Sedick Gallie for his assistance with sampling and for conducting the microscope counts, and Raquel Flynn, Mishka Rawatlal, and Raymond Roman for assistance with nutrient analyses. We acknowledge the Flow Cytometry Core Facility at the University of Cape Town (UCT) and the efforts of Ian Newton at the Stable Light Isotope Laboratory (UCT). This work was supported by the South African Departments of Forestry, Fisheries, and Environment (formerly Environmental Affairs) and Science and Innovation (DSI), and the National Research Foundation (NRF) through the South African National Antarctic Program (SANAP; 110732 to K.E.A and 105539, 110735, and 129232 to S.E.F.), Equipment-related Travel and Training Grant (118615 to K.E.A.), Competitive Support for Rated Researchers Grant (111716 to K.E.A.), and Incentive Fund (115335 to S.E.F.). S.S., M.M., K.A.M.S., and J.M.B. acknowledge funding from the NRF through postgraduate scholarships (120105, 112380, 113193, and 108757, respectively). S.S. was partially supported by a UCT Vice-Chancellor Research Scholarship and M.M. by the UCT Harry Crossley Foundation Research Fellowship. S.E.F. and K.E.A. acknowledge the support of the UCT Vice-Chancellor Future Leaders 2030 programme. S.E.F. acknowledges an African Academy of Sciences/Royal Society FLAIR fellowship and K.E.A. acknowledges support from UCT through a University Research Council Launching Grant and a University Equipment Committee Grant. We further acknowledge the support of the DSI Biogeochemistry Research Infrastructure Platform (BIOGRIP).

7. References

Aarnos, H., Ylöstalo, P. and Vähätalo, A.V., (2012). Seasonal phototransformation of dissolved organic matter to ammonium, dissolved inorganic carbon, and labile substrates supporting bacterial biomass across the Baltic Sea. *Journal of Geophysical Research: Biogeosciences*, 117(G1).

Alldredge, A.L. and Gotschalk, C., (1988). In situ settling behavior of marine snow 1. *Limnology and Oceanography*, 33(3), pp.339-351.

Altieri, K.E., Spence, K.A.M., and Smith, S. (2021). Air-Sea Ammonia Fluxes Calculated from High-Resolution Summertime Observations Across the Atlantic Southern Ocean. *Geophysical Research Letters*.

Amin, S.A., Moffett, J.W., Martens-Habbena, W., Jacquot, J.E., Han, Y., Devol, A., Ingalls, A.E., Stahl, D.A. and Armbrust, E.V., (2013). Copper requirements of the ammonia-oxidizing archaeon Nitrosopumilus maritimus SCM1 and implications for nitrification in the marine environment. *Limnology and Oceanography*, 58(6), pp.2037-2045.

Armstrong, R.A., (1999). An optimization-based model of iron-light-ammonium colimitation of nitrate uptake and phytoplankton growth. *Limnology and Oceanography*, 44(6), pp.1436-1446.

Arrigo, K. R., van Dijken, G. L., and Bushinsky, S. (2008). Primary production in the Southern Ocean, 1997–2006. *Journal of Geophysical Research*, *113*(C8), C08004.

Arteaga, L.A., Pahlow, M., Bushinsky, S.M. and Sarmiento, J.L., (2019). Nutrient controls on export production in the Southern Ocean. *Global Biogeochemical Cycles*, 33(8), pp.942-956.

https://doi.org/10.5194/bg-2021-149
Preprint. Discussion started: 10 June 2021

959 Baer, S.E., Connelly, T.L., Sipler, R.E., Yager, P.L. and Bronk, D.A., (2014). Effect of temperature on rates of ammonium
960 uptake and nitrification in the western coastal Arctic during winter, spring, and summer. *Global Biogeochemical Cycles*,
961 *28*(12), pp.1455-1466.

962 Bagwell, J.E., (2009). Transcriptional Response of Nitrogen Uptake and Assimilation in Marine Diatoms; Thalassiosira
963 Pseudonana and Thalassiosira Weissflogii (Doctoral dissertation, University of North Carolina Wilmington).

964 Baird, M.E., Emsley, S.M. and Mcglade, J.M., (2001). Modelling the interacting effects of nutrient uptake, light capture
965 and temperature on phytoplankton growth. *Journal of Plankton Research*, *23*(8), pp.829-840.

966 Barlow, R.G., and Alberte, R.S., (1985). Photosynthetic characteristics of phycoerythrin-containing marine
967 Synechococcus spp.. *Marine Biology* 86, 63–74.

968 Bathmann, U.V., Scharek, R., Klaas, C., Dubischar, C.D. and Smetacek, V., (1997). Spring development of phytoplankton
969 biomass and composition in major water masses of the Atlantic sector of the Southern Ocean. Deep Sea Research Part II:
970 Topical Studies in Oceanography, 44(1-2), pp.51-67.

971 Becquevort, S., Menon, P., and Lancelot, C. (2000). Differences of the protozoan biomass and grazing during spring and
972 summer in the Indian sector of the Southern Ocean. *Polar Biology*, *23*(5), 309–320.

973 Belkin, I. M., and Gordon, A. L. (1996). Southern Ocean fronts from the Greenwich meridian to Tasmania. *Journal of*
974 *Geophysical Research C: Oceans*, 101(C2), 3675–3696.

975 Bendschneider, K. and Robinson, R.J., (1952). A new spectrophotometric method for the determination of nitrite in sea
976 water.

977 Bianchi, M., Feliatra, F., Tréguer, P., Vincendeau, M.A. and Morvan, J., (1997). Nitrification rates, ammonium and nitrate
978 distribution in upper layers of the water column and in sediments of the Indian sector of the Southern Ocean. *Deep Sea*
979 *Research Part II: Topical Studies in Oceanography*, *44*(5), pp.1017-1032.

980 Bouwman, A. F., Lee, D. S., Asman, W. A. H., Dentener, F. J., Van Der Hoek, K. W., and Olivier, J. G. J. (1997). A
981 global high-resolution emission inventory for ammonia. *Global Biogeochemical Cycles*, *11*(4), 561–587.

982 Boyd, P.W., Crossley, A.C., DiTullio, G.R., Griffiths, F.B., Hutchins, D.A., Queguiner, B., Sedwick, P.N. and Trull,
983 T.W., (2001). Control of phytoplankton growth by iron supply and irradiance in the subantarctic Southern Ocean:
984 Experimental results from the SAZ Project. *Journal of Geophysical Research: Oceans*, *106*(C12), pp.31573-31583.

985 Boyd, P. W., Rynearson, T. A., Armstrong, E. A., Fu, F., Hayashi, K., Hu, Z., Hutchins, D. A., Kudela, R. M., Litchman,
986 E., Mulholland, M. R., Passow, U., Strzepek, R. F., Whittaker, K. A., Yu, E., and Thomas, M. K. (2013). Marine
987 Phytoplankton Temperature versus Growth Responses from Polar to Tropical Waters - Outcome of a Scientific
988 Community-Wide Study. *PLoS ONE*, *8*(5), 1–17.

989 Bracher, A. U., Kroon, B. M. A., and Lucas, M. I. (1999). Primary production, physiological state and composition of
990 phytoplankton in the Atlantic sector of the Southern Ocean. *Marine Ecology Progress Series*, *190*, 1–16.

991 Brightman, R.I. and Smith Jr, W.O., (1989). Photosynthesis-irradiance relationships of Antarctic phytoplankton during
992 austral winter. *Marine Ecology Progress Series*, pp.143-151.

993 Brzezinski, M. A. (1988). Vertical distribution of ammonium in stratified oligotrophic waters. *Limnol. Oceanogr.* 33(5),
994 1176–1182.

995 Buongiorno Nardelli, B., Guinehut, S., Verbrugge, N., Cotroneo, Y., Zambianchi, E. and Iudicone, D., (2017). Southern
996 Ocean mixed-layer seasonal and interannual variations from combined satellite and in situ data. *Journal of Geophysical*
997 *Research: Oceans*, *122*(12), pp.10042-10060.

998 Campitelli E. (2019). metR: Tools for Easier Analysis of Meteorological Fields. R package version 0.5.0.
999 https://CRAN.R-project.org/package=metR

1000 Capone, D.G., Bronk, D.A., Mulholland, M.R. and Carpenter, E.J. eds., (2008). *Nitrogen in the marine environment*.
1001 Elsevier.

1002 Carvalho, F., Kohut, J., Oliver, M.J. and Schofield, O., (2017). Defining the ecologically relevant mixed-layer depth for
1003 Antarctica's coastal seas. *Geophysical Research Letters*, *44*(1), pp.338-345.

1004 Casey, J.R., Lomas, M.W., Michelou, V.K., Dyhrman, S.T., Orchard, E.D., Ammerman, J.W. and Sylvan, J.B., (2009).
1005 Phytoplankton taxon-specific orthophosphate (Pi) and ATP utilization in the western subtropical North Atlantic. *Aquatic*
1006 *microbial ecology*, 58(1), pp.31-44.

1007 Cavalieri, D.J. and Parkinson, C.L., (2008). Antarctic sea ice variability and trends, 1979–2006. *Journal of Geophysical*
1008 *Research: Oceans*, 113(C7).

1009 Checkley Jr, D.M. and Miller, C.A., (1989). Nitrogen isotope fractionation by oceanic zooplankton. *Deep Sea Research*
1010 *Part A. Oceanographic Research Papers*, 36(10), pp.1449-1456.

1011 Chisholm, S. W. (1992). Phytoplankton Size. In *Primary Productivity and Biogeochemical Cycles in the Sea* (pp. 213–
1012 237). Springer US.

https://doi.org/10.5194/bg-2021-149
Preprint. Discussion started: 10 June 2021

1013 Church, M.J., DeLong, E.F., Ducklow, H.W., Karner, M.B., Preston, C.M. and Karl, D.M., (2003). Abundance and
1014 distribution of planktonic Archaea and Bacteria in the waters west of the Antarctic Peninsula. *Limnology and*
1015 *Oceanography*, *48*(5), pp.1893-1902.

1016 Coale, K. H., Gordon, R. M., and Wang, X. (2005). The distribution and behaviour of dissolved and particulate iron and
1017 zinc in the Ross Sea and Antarctic circumpolar current along 170°W. *Deep-Sea Research Part I: Oceanographic*
1018 *Research Papers*, *52*(2), 295–318.

1019 Cochlan, W.P., (1986). Seasonal study of uptake and regeneration of nitrogen on the Scotian Shelf. Continental Shelf
1020 Research, 5(5), pp.555-577.

1021 Cochlan, W.P., (2008). Nitrogen uptake in the Southern Ocean. *Nitrogen in the Marine Environment*, edited by: Capone,
1022 DG, Bronk, DA, Mulholland, MR, and Carpenter, EJ, 2nd Edition, Academic Press, Elsevier, pp.569-596.

1023 Cochlan, W.P., Bronk, D.A. and Coale, K.H., (2002). Trace metals and nitrogenous nutrition of Antarctic phytoplankton:
1024 experimental observations in the Ross Sea. *Deep Sea Research Part II: Topical Studies in Oceanography*, 49(16),
1025 pp.3365-3390.

1026 Coello-Camba, A. and Agustí, S., (2017). Thermal thresholds of phytoplankton growth in polar waters and their
1027 consequences for a warming polar ocean. *Frontiers in Marine Science*, *4*, p.168.

1028 Cota, G.F., Smith, W.O., Nelson, D.M., Muench, R.D. and Gordon, L.I., (1992). Nutrient and biogenic particulate
1029 distributions, primary productivity and nitrogen uptake in the Weddell-Scotia Sea marginal ice zone during winter.
1030 *Journal of Marine Research*, *50*(1), pp.155-181

1031 Daly, K. L., Smith, W. O., Johnson, G. C., DiTullio, G. R., Jones, D. R., Mordy, C. W., Feely, R. A., Hansell, D. A., and
1032 Zhang, J.-Z. (2001). Hydrography, nutrients, and carbon pools in the Pacific sector of the Southern Ocean: Implications
1033 for carbon flux. *Journal of Geophysical Research: Oceans*, *106*(C4), 7107–7124.

1034 Deary, A. (2020). A high-resolution study of the early- to late summer progression in primary production and carbon
1035 export potential in the Atlantic Southern Ocean. (Honours thesis, University of Cape Town).

1036 del Giorgio, P.A. and Cole, J.J., (1998). Bacterial growth efficiency in natural aquatic systems. *Annual Review of Ecology*
1037 *and Systematics*, 29(1), pp.503-541.

1038 Dennett, M. R., Mathot, S., Caron, D. A., Smith, W. O., and Lonsdale, D. J. (2001). Abundance and distribution of
1039 phototrophic and heterotrophic nano- and microplankton in the southern Ross Sea. *Deep-Sea Research Part II: Topical*
1040 *Studies in Oceanography*, *48*(19–20), 4019–4037.

1041 Deppeler, S.L. and Davidson, A.T., (2017). Southern Ocean phytoplankton in a changing climate. *Frontiers in Marine*
1042 *Science*, 4, p.40.

1043 Detmer, A.E. and Bathmann, U.V., (1997). Distribution patterns of autotrophic pico-and nanoplankton and their relative
1044 contribution to algal biomass during spring in the Atlantic sector of the Southern Ocean. *Deep Sea Research Part II:*
1045 *Topical Studies in Oceanography*, *44*(1-2), pp.299-320.

1046 DiFiore, P. J., Sigman, D. M., Trull, T. W., Lourey, M. J., Karsh, K., Cane, G., and Ho, R. (2006). Nitrogen isotope
1047 constraints on subantarctic biogeochemistry. *Journal of Geophysical Research: Oceans*, *111*(8).
1048 https://doi.org/10.1029/2005JC003216

1049 DiFiore, P. J., Sigman, D. M., and Dunbar, R. B. (2009). Upper ocean nitrogen fluxes in the Polar Antarctic Zone:
1050 Constraints from the nitrogen and oxygen isotopes of nitrate. *Geochemistry, Geophysics, Geosystems*, *10*(11).

1051 DiFiore, P.J., Sigman, D.M., Karsh, K.L., Trull, T.W., Dunbar, R.B. and Robinson, R.S., (2010). Poleward decrease in the
1052 isotope effect of nitrate assimilation across the Southern Ocean. *Geophysical Research Letters*, 37(17).

1053 Dixon, G.K. and Syrett, P.J., (1988). The growth of dinoflagellates in laboratory cultures. *New phytologist*, *109*(3),
1054 pp.297-302.

1055 Doney, S.C., Mahowald, N., Lima, I., Feely, R.A., Mackenzie, F.T., Lamarque, J.F. and Rasch, P.J., (2007). Impact of
1056 anthropogenic atmospheric nitrogen and sulfur deposition on ocean acidification and the inorganic carbon
1057 system. *Proceedings of the National Academy of Sciences*, *104*(37), pp.14580-14585.

1058 Dong, S., Sprintall, J., Gille, S.T. and Talley, L., (2008). Southern Ocean mixed-layer depth from Argo float profiles.
1059 *Journal of Geophysical Research: Oceans*, *113*(C6).

1060 Dortch, Q. (1990). The interaction between ammonium and nitrate uptake in phytoplankton. *Marine Ecology Progress*
1061 *Series*, *61*(1), 183–201.

1062 Dugdale, R. C., and Goering, J. J. (1967). Uptake of new and regenerated forms of nitrogen in primary productivity.
1063 *Limnology and Oceanography*, *12*(2), 196–206.

1064 Dugdale, R.C. and Wilkerson, F.P., (1986). The use of 15N to measure nitrogen uptake in eutrophic oceans; experimental
1065 considerations 1, 2. *Limnology and Oceanography*, *31*(4), pp.673-689.

1066 Ellwood, M.J., Boyd, P.W. and Sutton, P., (2008). Winter-time dissolved iron and nutrient distributions in the
1067 Subantarctic Zone from 40–52S; 155–160E. *Geophysical Research Letters*, 35(11).

https://doi.org/10.5194/bg-2021-149
Preprint. Discussion started: 10 June 2021

1068 El-Sayed, S., (1984). Productivity of the Antarctic waters—a reappraisal. In *Marine phytoplankton and productivity* (pp.
1069 19-34). Springer, Berlin, Heidelberg.

1070 El-Sayed, S.Z. and Taguchi, S., (1981). Primary production and standing crop of phytoplankton along the ice-edge in the
1071 Weddell Sea. *Deep Sea Research Part A. Oceanographic Research Papers*, *28*(9), pp.1017-1032.

1072 Eppley, R.W., (1972). Temperature and phytoplankton growth in the sea. *Fish. bull*, *70*(4), pp.1063-1085.

1073 Eppley, R.W. and Peterson, B.J., (1979). Particulate organic matter flux and planktonic new production in the deep
1074 ocean. *Nature*, *282*(5740), pp.677-680.

1075 Fan, C., Glibert, P.M., and Burkholder, J.M., (2003). Characterization of the affinity for nitrogen, uptake kinetics, and
1076 environmental relationships for Prorocentrum minimum in natural blooms and laboratory cultures. *Harmful Algae*, *2*(4),
1077 pp.283-299.

1078 Fiala, M. and Oriol, L., (1990). Light-temperature interactions on the growth of Antarctic diatoms. *Polar Biology*, *10*(8),
1079 pp.629-636.

1080 Fiala, M., Semeneh, M. and Oriol, L., (1998). Size-fractionated phytoplankton biomass and species composition in the
1081 Indian sector of the Southern Ocean during austral summer. *Journal of Marine Systems*, *17*(1-4), pp.179-194.

1082 Finkel, Z.V., Irwin, A.J. and Schofield, O., (2004). Resource limitation alters the 3/4 size scaling of metabolic rates in
1083 phytoplankton. *Marine Ecology Progress Series*, *273*, pp.269-279.

1084 Finley A., Banerjee S., and Hjelle Ø. (2017). MBA: Multilevel B-Spline Approximation. package version 0.0-9.
1085 https://CRAN.R-project.org/package=MBA

1086 Flynn, R.F., Burger, J.M., Pillay, K. and Fawcett, S.E., (2018). Wintertime rates of net primary production and nitrate and
1087 ammonium uptake in the southern Benguela upwelling system. *African Journal of Marine Science*, 40(3), pp.253-266.

1088 Franck, V.M., Brzezinski, M.A., Coale, K.H. and Nelson, D.M., (2000). Iron and silicic acid concentrations regulate Si
1089 uptake north and south of the Polar Frontal Zone in the Pacific Sector of the Southern Ocean. *Deep Sea Research Part II:*
1090 *Topical Studies in Oceanography*, *47*(15-16), pp.3315-3338.

1091 Franck, V.M., Smith, G.J., Bruland, K.W. and Brzezinski, M.A., (2005). Comparison of size-dependent carbon, nitrate,
1092 and silicic acid uptake rates in high-and low-iron waters. *Limnology and Oceanography*, 50(3), pp.825-838.

1093 Francois, R., Altabet, M.A. and Burckle, L.H., (1992). Glacial to interglacial changes in surface nitrate utilization in the
1094 Indian sector of the Southern Ocean as recorded by sediment δ15N. *Paleoceanography*, *7*(5), pp.589-606.

1095 Fransson, A., Chierici, M., Anderson, L. and David, R., (2004). Transformation of carbon and oxygen in the surface layer
1096 of the eastern Atlantic sector of the Southern Ocean. *Deep Sea Research Part II: Topical Studies in Oceanography*, *51*(22-
1097 24), pp.2757-2772.

1098 Frigstad, H., Andersen, T., Hessen, D.O., Naustvoll, L.J., Johnsen, T.M. and Bellerby, R.G., (2011). Seasonal variation in
1099 marine C: N: P stoichiometry: can the composition of seston explain stable Redfield ratios?. *Biogeosciences*, 8(10),
1100 pp.2917-2933.

1101 Froneman, P.W., Ansorge, I.J., Pakhomov, E.A. and Lutjeharms, J.R.E., (1999). Plankton community structure in the
1102 physical environment surrounding the Prince Edward Islands (Southern Ocean). *Polar Biology*, *22*(3), pp.145-155.

1103 Fujiki, T. and Taguchi, S., (2002). Variability in chlorophyll a specific absorption coefficient in marine phytoplankton as a
1104 function of cell size and irradiance. *Journal of Plankton Research*, *24*(9), pp.859-874.

1105 Gao, Y., Kaufman, Y. J., Tanré, D., Kolber, D., and Falkowski, P. G. (2001). Seasonal distributions of aeolian iron fluxes
1106 to the global ocean. *Geophysical Research Letters*, *28*(1), pp.29–32.

1107 Gasol, J.M. and Del Giorgio, P.A., (2000). Using flow cytometry for counting natural planktonic bacteria and
1108 understanding the structure of planktonic bacterial communities. *Scientia Marina*, 64(2), pp.197-224.

1109 Glibert, P.M., (1982). Regional studies of daily, seasonal and size fraction variability in ammonium remineralization.
1110 *Marine Biology*, 70(2), pp.209-222.

1111 Glibert, P. M., Wilkerson, F. P., Dugdale, R. C., Raven, J. A., Dupont, C. L., Leavitt, P. R., Parker, A. E., Burkholder, J.
1112 M., and Kana, T. M. (2016). Pluses and minuses of ammonium and nitrate uptake and assimilation by phytoplankton and
1113 implications for productivity and community composition, with emphasis on nitrogen-enriched conditions. *Limnology and*
1114 *Oceanography*, *61*(1), pp.165–197.

1115 Goericke, R., (1998). Response of phytoplankton community structure and taxon-specific growth rates to seasonally
1116 varying physical forcing in the Sargasso Sea off Bermuda. *Limnology and Oceanography*, *43*(5), pp.921-935.

1117 Goeyens, L., Tréguer, P., Lancelot, C., Mathot, S., Becquevort, S., Morvan, J., Dehairs, F. and Baeyens, W., (1991).
1118 Ammonium regeneration in the Scotia-Weddell Confluence area during spring 1988. *Marine Ecology Progress Series*,
1119 pp.241-252.

1120 Goeyens, L., Tréguer, P., Baumann, M. E. M., Baeyens, W., and Dehairs, F. (1995). The leading role of ammonium in the
1121 nitrogen uptake regime of Southern Ocean marginal ice zones. *Journal of Marine Systems*, *6*(4), pp.345–361.

https://doi.org/10.5194/bg-2021-149
Preprint. Discussion started: 10 June 2021

1122 Greene, R.M., Geider, R.J. and Falkowski, P.G., (1991). Effect of iron limitation on photosynthesis in a marine diatom.
1123 *Limnology and Oceanography*, *36*(8), pp.1772-1782.

1124 Harrison, W.G., (1976). Nitrate metabolism of the red tide dinoflagellate Gonyaulax polyedra Stein. *Journal of*
1125 *Experimental Marine Biology and Ecology*, *21*(3), pp.199-209.

1126 Hasle, R.G., (1978). The inverted microscope method. *Phytoplankton manual*, pp.88-96.

1127 Henley, S.F., Tuerena, R.E., Annett, A.L., Fallick, A.E., Meredith, M.P., Venables, H.J., Clarke, A. and Ganeshram, R.S.,
1128 (2017). Macronutrient supply, uptake and recycling in the coastal ocean of the west Antarctic Peninsula. *Deep Sea*
1129 *Research Part II: Topical Studies in Oceanography*, 139, pp.58-76.

1130 Hense, I., Bathmann, U.V. and Timmermann, R., (2000). Plankton dynamics in frontal systems of the Southern
1131 Ocean. *Journal of Marine Systems*, *27*(1-3), pp.235-252.

1132 Herbert, R.A., (1999). Nitrogen cycling in coastal marine ecosystems. *FEMS microbiology reviews*, *23*(5), pp.563-590.

1133 Hewes, C.D., Holm-Hansen, O. and Sakshaug, E., (1985). Alternate carbon pathways at lower trophic levels in the
1134 Antarctic food web. *Antarctic nutrient cycles and food webs*. pp. 277-28.

1135 Hiscock, M.R., Marra, J., Smith Jr, W.O., Goericke, R., Measures, C., Vink, S., Olson, R.J., Sosik, H.M. and Barber, R.T.,
1136 (2003). Primary productivity and its regulation in the Pacific Sector of the Southern Ocean. *Deep Sea Research Part II:*
1137 *Topical Studies in Oceanography*, 50(3-4), pp.533-558.

1138 Holm-Hansen, O., Hewes, C.D., Villafane, V.E., Helbling, E.W., Silva, N. and Amos, T., (1997). Distribution of
1139 phytoplankton and nutrients in relation to different water masses in the area around Elephant Island, Antarctica. *Polar*
1140 *Biology*, *18*(2), pp.145-153.

1141 Holmes, R.M., Aminot, A., Kérouel, R., Hooker, B.A. and Peterson, B.J., (1999). A simple and precise method for
1142 measuring ammonium in marine and freshwater ecosystems. *Canadian Journal of Fisheries and Aquatic Sciences*, *56*(10),
1143 pp.1801-1808.

1144 Holzer, M., Primeau, F.W., DeVries, T. and Matear, R., (2014). The Southern Ocean silicon trap: Data-constrained
1145 estimates of regenerated silicic acid, trapping efficiencies, and global transport paths. *Journal of Geophysical Research:*
1146 *Oceans*, *119*(1), pp.313-331.

1147 Honjo, S., Francois, R., Manganini, S., Dymond, J. and Collier, R., (2000). Particle fluxes to the interior of the Southern
1148 Ocean in the Western Pacific sector along 170 W. *Deep Sea Research Part II: Topical Studies in Oceanography*, *47*(15-
1149 16), pp.3521-3548.

1150 Hooper, A.B. and Terry, K.R., (1974). Photoinactivation of ammonia oxidation in Nitrosomonas. *Journal of Bacteriology*,
1151 119(3), pp.899-906.

1152 Horrigan, S. G., & Springer, A. L. (1990). Oceanic and estuarine ammonium oxidation: Effects of light. *Limnology and*
1153 *Oceanography*, *35*(2), pp.479–482.

1154 Huang, K., Feng, Q., Zhang, Y., Ou, L., Cen, J., Lu, S. and Qi, Y., (2020). Comparative uptake and assimilation of nitrate,
1155 ammonium, and urea by dinoflagellate Karenia mikimotoi and diatom Skeletonema costatum sl in the coastal waters of the
1156 East China Sea. *Marine Pollution Bulletin*, *155*, p.111200.

1157 Hudson, R.J. and Morel, F.M., (1993). Trace metal transport by marine microorganisms: implications of metal
1158 coordination kinetics. *Deep Sea Research Part I: Oceanographic Research Papers*, *40*(1), pp.129-150.

1159 Hutchins, D.A., Sedwick, P.N., DiTullio, G.R., Boyd, P.W., Queguiner, B., Griffiths, F.B. and Crossley, C., (2001).
1160 Control of phytoplankton growth by iron and silicic acid availability in the subantarctic Southern Ocean: Experimental
1161 results from the SAZ Project. *Journal of Geophysical Research: Oceans*, *106*(C12), pp.31559-31572.

1162 Iida, T. and Odate, T., (2014). Seasonal variability of phytoplankton biomass and composition in the major water masses
1163 of the Indian Ocean sector of the Southern Ocean. *Polar Science*, *8*(3), pp.283-297.

1164 Jacobson, D. M., and Anderson, D. M. (1996). Widespread phagocytosis of ciliates and other protists by marine
1165 mixotrophic and heterotrophic thecate dinoflagellates. *Journal of Phycology*, *32*(2), 279–285.

1166 Janssen, D.J., Sieber, M., Ellwood, M.J., Conway, T.M., Barrett, P.M., Chen, X., de Souza, G.F., Hassler, C.S. and
1167 Jaccard, S.L., (2020). Trace metal and nutrient dynamics across broad biogeochemical gradients in the Indian and Pacific
1168 sectors of the Southern Ocean. *Marine chemistry*, *221*, p.103773.

1169 Jeong, H.J. and Latz, M.I., (1994). Growth and grazing rates of the heterotrophic dinoflagellates Protoperidinium spp. on
1170 red tide dinoflagellates. *Marine Ecology-Progress Series*, *106*, pp.173-173.

1171 Jiang, H.B., Fu, F.X., Rivero-Calle, S., Levine, N.M., Sañudo-Wilhelmy, S.A., Qu, P.P., Wang, X.W., Pinedo-Gonzalez,
1172 P., Zhu, Z. and Hutchins, D.A., (2018). Ocean warming alleviates iron limitation of marine nitrogen fixation. *Nature*
1173 *Climate Change*, *8*(8), pp.709-712.

1174 Johnson, K.S., Plant, J.N., Dunne, J.P., Talley, L.D. and Sarmiento, J.L., (2017). Annual nitrate drawdown observed by
1175 SOCCOM profiling floats and the relationship to annual net community production. *Journal of Geophysical Research:*
1176 *Oceans*, *122*(8), pp.6668-6683.

https://doi.org/10.5194/bg-2021-149
Preprint. Discussion started: 10 June 2021

1177 Johnson, M.T., Liss, P.S., Bell, T.G., Lesworth, T.J., Baker, A.R., Hind, A.J., Jickells, T.D., Biswas, K.F., Woodward,
1178 E.M.S. and Gibb, S.W., (2008). Field observations of the ocean-atmosphere exchange of ammonia: Fundamental
1179 importance of temperature as revealed by a comparison of high and low latitudes. *Global Biogeochemical Cycles*, 22(1).

1180 Jones, R.D., Morita, R.Y., Koops, H.P. and Watson, S.W., (1988). A new marine ammonium-oxidizing bacterium,
1181 Nitrosomonas cryotolerans sp. nov. *Canadian journal of microbiology*, *34*(10), pp.1122-1128.

1182 Joubert, W. R., Thomalla, S. J., Waldron, H. N., Lucas, M. I., Boye, M., Le Moigne, F. A. C., Planchon, F., and Speich, S.
1183 (2011). Nitrogen uptake by phytoplankton in the Atlantic sector of the Southern Ocean during late austral summer.
1184 *Biogeosciences*, *8*(10), pp.2947–2959.

1185 Kassambara A. (2019). ggpubr: 'ggplot2' Based Publication Ready Plots. R package version 0.2.4. https://CRAN.R-
1186 project.org/package=ggpubr

1187 Kattner, G., Thomas, D.N., Haas, C., Kennedy, H. and Dieckmann, G.S., (2004). Surface ice and gap layers in Antarctic
1188 sea ice: highly productive habitats. *Marine Ecology Progress Series*, 277, pp.1-12.

1189 Kirchman, D. L. (1994). The Uptake of Inorganic Nutrients by Heterotrophic Bacteria. *Microbial Ecology* 28(2), pp.255–
1190 71.

1191 Kitzinger, K., Padilla, C.C., Marchant, H.K., Hach, P.F., Herbold, C.W., Kidane, A.T., Könneke, M., Littmann, S.,
1192 Mooshammer, M., Niggemann, J. and Petrov, S., (2019). Cyanate and urea are substrates for nitrification by
1193 Thaumarchaeota in the marine environment. Nature microbiology, 4(2), pp.234-243.

1194 Klawonn, I., Bonaglia, S., Whitehouse, M.J., Littmann, S., Tienken, D., Kuypers, M.M., Brüchert, V. and Ploug, H.,
1195 (2019). Untangling hidden nutrient dynamics: rapid ammonium cycling and single-cell ammonium assimilation in marine
1196 plankton communities. *The ISME journa*l, 13(8), pp.1960-1974.

1197 Knapp, A.N., Dekaezemacker, J., Bonnet, S., Sohm, J.A. and Capone, D.G., (2012). Sensitivity of Trichodesmium
1198 erythraeum and Crocosphaera watsonii abundance and N2 fixation rates to varying NO3− and PO43− concentrations in
1199 batch cultures. *Aquatic microbial ecology*, 66(3), pp.223-236.

1200 Kobayashi, F. and Takahashi, K., (2002). Distribution of diatoms along the equatorial transect in the western and central
1201 Pacific during the 1999 La Niña conditions. *Deep Sea Research Part II: Topical Studies in Oceanography*, *49*(13-14),
1202 pp.2801-2821.

1203 Koike, I., Holm-Hansen, O., and Biggs, D. C. (1986). Phytoplankton With Special Reference To Ammonium Cycling.
1204 *Marine Ecology*, *30*, pp.105–116.

1205 Kopczynska, E.E., Weber, L.H. and El-Sayed, S.Z., (1986). Phytoplankton species composition and abundance in the
1206 Indian sector of the Antarctic Ocean. *Polar Biology*, *6*(3), pp.161-169.

1207 Kopczynska, E.E., Dehairs, F., Elskens, M. and Wright, S., (2001). Phytoplankton and microzooplankton variability
1208 between the Subtropical and Polar Fronts south of Australia: Thriving under regenerative and new production in late
1209 summer. *Journal of Geophysical Research: Oceans*, *106*(C12), pp.31597-31609.

1210 Kopczyńska, E. E., Savoye, N., Dehairs, F., Cardinal, D., and Elskens, M. (2007). Spring phytoplankton assemblages in
1211 the Southern Ocean between Australia and Antarctica. *Polar Biology*, *31*(1), pp.77–88.

1212 Kottmeier, S.T. and Sullivan, C.W., (1987). Late winter primary production and bacterial production in sea ice and
1213 seawater west of the Antarctic Peninsula. *Mar Ecol Prog Ser*, *36*, pp.287-298.

1214 Krell, A., Schnack-Schiel, S.B., Thomas, D.N., Kattner, G., Zipan, W. and Dieckmann, G.S., (2005). Phytoplankton
1215 dynamics in relation to hydrography, nutrients and zooplankton at the onset of sea ice formation in the eastern Weddell
1216 Sea (Antarctica). *Polar Biology*, 28(9), pp.700-713.

1217 Kristiansen, S. and Farbrot, T., (1991). Nitrogen uptake rates in phytoplankton and ice algae in the Barents Sea. *Polar*
1218 *research*, 10(1), pp.187-192.

1219 Kustka, A.B., Sañudo-Wilhelmy, S.A., Carpenter, E.J., Capone, D., Burns, J. and Sunda, W.G., (2003). Iron requirements
1220 for dinitrogen-and ammonium-supported growth in cultures of Trichodesmium (IMS 101): Comparison with nitrogen
1221 fixation rates and iron: Carbon ratios of field populations. *Limnology and Oceanography*, 48(5), pp.1869-1884.

1222 La Roche, J. (1983). Ammonium regeneration: its contribution to phytoplankton nitrogen requirements in a eutrophic
1223 environment. *Marine Biology*, *75*(2–3), pp.231–240.

1224 Landry, M.R., Selph, K.E., Brown, S.L., Abbott, M.R., Measures, C.I., Vink, S., Allen, C.B., Calbet, A., Christensen, S.
1225 and Nolla, H., (2002). Seasonal dynamics of phytoplankton in the Antarctic Polar Front region at 170° W. *Deep Sea*
1226 *Research Part II: Topical Studies in Oceanography*, *49*(9-10), pp.1843-1865.

1227 Laubscher, R.K., Perissinotto, R. and McQuaid, C.D., (1993). Phytoplankton production and biomass at frontal zones in
1228 the Atlantic sector of the Southern Ocean. *Polar biology*, *13*(7), pp.471-481.

1229 Lauderdale, J.M., Garabato, A.C.N., Oliver, K.I., Follows, M.J. and Williams, R.G., (2013). Wind-driven changes in
1230 Southern Ocean residual circulation, ocean carbon reservoirs and atmospheric CO 2. *Climate dynamics*, *41*(7-8), pp.2145-
1231 2164.

1232 Lee, S.H., Joo, H.M., Liu, Z., Chen, J. and He, J., (2012). Phytoplankton productivity in newly opened waters of the
1233 Western Arctic Ocean. *Deep Sea Research Part II: Topical Studies in Oceanography*, *81*, pp.18-27.

https://doi.org/10.5194/bg-2021-149
Preprint. Discussion started: 10 June 2021

1234 Lee, S.H., Yun, M.S., Kim, B.K., Joo, H., Kang, S.H., Kang, C.K. and Whitledge, T.E., (2013). Contribution of small
1235 phytoplankton to total primary production in the Chukchi Sea. *Continental Shelf Research*, *68*, pp.43-50.

1236 Lehette, P., Tovar-Sánchez, A., Duarte, C.M. and Hernández-León, S., (2012). Krill excretion and its effect on primary
1237 production. *Marine Ecology Progress Series*, *459*, pp.29-38.

1238 Le Moigne, F. A., Boye, M., Masson, A., Corvaisier, R., Grossteffan, E., Gueneugues, A., Pondaven, P., Le Moigne, F. A.
1239 C., Boye, M., Corvaisier, R., Guéneugues, A., & Pondaven, P. (2013). Description of the biogeochemical features of the
1240 subtropical southeastern Atlantic and the Southern Ocean south of South Africa during the austral summer of the
1241 International Polar Year. *European Geosciences Union*, *10*(10), pp.281–295.

1242 Lin, C. T., Jickells, T. D., Baker, A. R., Marca, A., & Johnson, M. T. (2016). Aerosol isotopic ammonium signatures over
1243 the remote Atlantic Ocean. *Atmospheric Environment*, *133*, pp.165–169.

1244 Lipschultz, F., (2008). Isotope tracer methods for studies of the marine nitrogen cycle. *Nitrogen in the Marine*
1245 *Environment*, 2nd Edition, Academic Press: Burlington, MA, USA, pp.1345-1384.

1246 Llort, J., Lévy, M., Sallée, J.B., and Tagliabue, A., (2019). Nonmonotonic response of primary production and export to
1247 changes in mixed-layer depth in the Southern Ocean. *Geophysical Research Letters*, *46*(6), pp.3368-3377.

1248 Longhurst, A. R. (1998). Ecological Geography of the Sea. Academic Press, San Diego, CA.

1249 Lourey, M. J., Trull, T. W., and Sigman, D. M. (2003). Sensitivity of δ 15 N of nitrate, surface suspended and deep
1250 sinking particulate nitrogen to seasonal nitrate depletion in the Southern Ocean . *Global Biogeochemical Cycles*, *17*(3).

1251 Lu, S., Liu, X., Liu, C., Cheng, G., and Shen, H., (2020). Influence of photoinhibition on nitrification by ammonia-
1252 oxidizing microorganisms in aquatic ecosystems. *Reviews in Environmental Science and Bio/Technology*, pp.1-12.

1253 Lutjeharms, J. R. E., and Valentine, H. R. (1984). Southern ocean thermal fronts south of Africa. *Deep Sea Research Part*
1254 *A, Oceanographic Research Papers*, *31*(12), 1461–1475.

1255 Macko, S.A., Estep, M.L.F., Engel, M.H., and Hare, P.E., (1986). Kinetic fractionation of stable nitrogen isotopes during
1256 amino acid transamination. *Geochimica et Cosmochimica Acta*, 50(10), pp.2143-2146.

1257 Marie, D., Partensky, F., Jacquet, S., and Vaulot, D., (1997). Enumeration and cell cycle analysis of natural populations of
1258 marine picoplankton by flow cytometry using the nucleic acid stain SYBR Green I. *Appl. Environ. Microbiol.*, *63*(1),
1259 pp.186-193.

1260 Marie, D., Simon, N., and Vaulot, D., (2005). Phytoplankton cell counting by flow cytometry. *Algal culturing*
1261 *techniques*, *1*, pp.253-267.

1262 Martin, J.H., Fitzwater, S.E., and Gordon, R.M., (1990). Iron deficiency limits phytoplankton growth in Antarctic
1263 waters. *Global Biogeochemical Cycles*, *4*(1), pp.5-12.

1264 Mayzaud, P., Razouls, S., Errhif, A., Tirelli, V. and Labat, J.P., (2002). Feeding, respiration and egg production rates of
1265 copepods during austral spring in the Indian sector of the Antarctic Ocean: role of the zooplankton community in carbon
1266 transformation. *Deep Sea Research Part I: Oceanographic Research Papers*, 49(6), pp.1027-1048.

1267 Mdutyana, M., Thomalla, S.J., Philibert, R., Ward, B.B., and Fawcett, S.E., (2020). The seasonal cycle of nitrogen uptake
1268 and nitrification in the Atlantic sector of the Southern Ocean. *Global Biogeochemical Cycles*, *34*(7), p.e2019GB006363.

1269 Mdutyana, M., (2021). Mixed layer nitrogen cycling in the Southern Ocean: seasonality, kinetics, and biogeochemical
1270 implications. (PhD dissertation, University of Cape Town).

1271 Mei, Z.P., Finkel, Z.V., and Irwin, A.J., (2009). Light and nutrient availability affect the size-scaling of growth in
1272 phytoplankton. *Journal of theoretical biology*, *259*(3), pp.582-588.

1273 Mengesha, S., Dehairs, F., Fiala, M., Elskens, M., and Goeyens, L. (1998). Seasonal variation of phytoplankton
1274 community structure and nitrogen uptake regime in the Indian Sector of the Southern Ocean. *Polar Biology*, *20*(4),
1275 pp.259–272.

1276 Möbius, J., (2013). Isotope fractionation during nitrogen remineralization (ammonification): Implications for nitrogen
1277 isotope biogeochemistry. *Geochimica et Cosmochimica Acta*, *105*, pp.422-432.

1278 Moore, J.K. and Abbott, M.R., (2000). Phytoplankton chlorophyll distributions and primary production in the Southern
1279 Ocean. *Journal of Geophysical Research: Oceans*, *105*(C12), pp.28709-28722.

1280 Mordy, C.W., Penny, D.M. and Sullivan, C.W., (1995). Spatial distribution of bacterioplankton biomass and production in
1281 the marginal ice-edge zone of the Weddell-Scotia Sea during austral winter. *Marine Ecology Progress Series*, *122*, pp.9-
1282 19.

1283 Mtshali, T.N., van Horsten, N.R., Thomalla, S.J., Ryan-Keogh, T.J., Nicholson, S.A., Roychoudhury, A.N., Bucciarelli,
1284 E., Sarthou, G., Tagliabue, A. and Monteiro, P.M., (2019). Seasonal depletion of the dissolved iron reservoirs in the sub-
1285 Antarctic zone of the Southern Atlantic Ocean. *Geophysical Research Letters*, *46*(8), pp.4386-4395.

1286 Munk, W.H., and Riley, G., (1952). Absorption of nutrients by aquatic plants. *Journal of Marine Research,* 11, pp. 215-
1287 240.

https://doi.org/10.5194/bg-2021-149
Preprint. Discussion started: 10 June 2021

1288 Murphy, J., and Riley, J.P., (1962). A modified single solution method for the determination of phosphate in natural
1289 waters. *Analytica chimica acta*, *27*, pp.31-36.

1290 Nelson, D.M., Brzezinski, M.A., Sigmon, D.E. and Franck, V.M., (2001). A seasonal progression of Si limitation in the
1291 Pacific sector of the Southern Ocean. *Deep Sea Research Part II: Topical Studies in Oceanography*, *48*(19-20), pp.3973-
1292 3995.

1293 Olson, R.J. (1981). Differential photoinhibition of marine nitrifying bacteria: a possible mechanism for the formation of
1294 the primary nitrite maximum.

1295 Orsi, A. H., Whitworth, T., and Nowlin, W. D. (1995). On the meridional extent and fronts of the Antarctic Circumpolar
1296 Current. *Deep-Sea Research Part I*, *42*(5), pp.641–673.

1297 Owens, N.J.P., Priddle, J. and Whitehouse, M.J., (1991). Variations in phytoplanktonic nitrogen assimilation around South
1298 Georgia and in the Bransfield Strait (Southern Ocean). *Marine Chemistry*, 35(1-4), pp.287-304.

1299 Pachiadaki, M.G., Sintes, E., Bergauer, K., Brown, J.M., Record, N.R., Swan, B.K., Mathyer, M.E., Hallam, S.J., Lopez-
1300 Garcia, P., Takaki, Y. and Nunoura, T., (2017). Major role of nitrite-oxidizing bacteria in dark ocean carbon
1301 fixation. *Science*, *358*(6366), pp.1046-1051.

1302 Painter, S.C., Patey, M.D., Tarran, G.A. and Torres-Valdés, S., (2014). Picoeukaryote distribution in relation to nitrate
1303 uptake in the oceanic nitracline. *Aquatic Microbial Ecology*, 72(3), pp.195-213.

1304 Palenik, B., Brahamsha, B., Larimer, F. W., Land, M., Hauser, L., Chain, P., Lamerdin, J., Regala, W., Allen, E. E.,
1305 McCarren, J., Paulsen, I., Dufresne, A., Partensky, F., Webb, E. A., and Waterbury, J., (2003). The genome of a motile
1306 marine Synechococcus. *Nature*, *424*(6952), 1037–1042.

1307 Paulot, F., Jacob, D. J., and Henze, D. K., (2013). Sources and processes contributing to nitrogen deposition: An adjoint
1308 model analysis applied to biodiversity hotspots worldwide. *Environmental Science and Technology*, *47*(7), pp.3226–3233.

1309 Paulot, F., Jacob, D. J., Johnson, M. T., Bell, T. G., Baker, A. R., Keene, W. C., Lima, I. D., Doney, S. C., and Stock, C.
1310 A., (2015). Global oceanic emission of ammonia: Constraints from seawater and atmospheric observations. *Global*
1311 *Biogeochemical Cycles*, *29*(8), pp.1165–1178.

1312 Pausch, F., Bischof, K. and Trimborn, S., (2019). Iron and manganese co-limit growth of the Southern Ocean diatom
1313 Chaetoceros debilis. *Plos one*, *14*(9), p.e0221959.

1314 Peng, X., Fuchsman, C.A., Jayakumar, A., Oleynik, S., Martens-Habbena, W., Devol, A.H. and Ward, B.B., (2015).
1315 Ammonia and nitrite oxidation in the Eastern Tropical North Pacific. *Global Biogeochemical Cycles*, *29*(12), pp.2034-
1316 2049.

1317 Philibert, R., Waldron, H. and Clark, D., (2015). A geographical and seasonal comparison of nitrogen uptake by
1318 phytoplankton in the Southern Ocean. *Ocean Science*, *11*(2).

1319 Pomeroy, L. R., and Wiebe, W. J. (2001). Temperature and substrates as interactive limiting factors for marine
1320 heterotrophic bacteria. *Aquatic Microbial Ecology*, *23*(2), pp.187–204.

1321 Prézelin, B.B., Hofmann, E.E., Mengelt, C. and Klinck, J.M., (2000). The linkage between Upper Circumpolar Deep
1322 Water (UCDW) and phytoplankton assemblages on the west Antarctic Peninsula continental shelf. *Journal of Marine*
1323 *Research*, 58(2), pp.165-202.

1324 Price, N.M., Ahner, B.A. and Morel, F.M., (1994). The equatorial Pacific Ocean: Grazer-controlled phytoplankton
1325 populations in an iron-limited ecosystem 1. *Limnology and Oceanography*, 39(3), pp.520-534.

1326 Primeau, F. W., Holzer, M., and DeVries, T. (2013). Southern Ocean nutrient trapping and the efficiency of the biological
1327 pump. *Journal of Geophysical Research: Oceans*, *118*(5), pp.2547–2564.

1328 R Core Team (2020). R: A language and environment for statistical computing. R Foundation for Statistical Computing,
1329 Vienna, Austria. URL https://www.R-project.org/.

1330 Raven, J.A., (1988). The iron and molybdenum use efficiencies of plant growth with different energy, carbon and nitrogen
1331 sources. *New Phytologist*, *109*(3), pp.279-287.

1332 Reay, D. S., Priddle, J., Nedwell, D. B., Whitehouse, M. J., Ellis-Evans, J. C., Deubert, C., and Connelly, D. P. (2001).
1333 Regulation by low temperature of phytoplankton growth and nutrient uptake in the Southern Ocean. *Marine Ecology*
1334 *Progress Series*, *219*(1990), pp.51–64.

1335 Rees, A., Woodward, M. and Joint, I., (1999). Measurement of nitrate and ammonium uptake at ambient concentrations in
1336 oligotrophic waters of the North-East Atlantic Ocean. *Marine Ecology Progress Series*, 187, pp.295-300.

1337 Rembauville, M., Briggs, N., Ardyna, M., Uitz, J., Catala, P., Penkerc'h, C., Poteau, A., Claustre, H., and Blain, S., (2017).
1338 Plankton assemblage estimated with BGC-Argo floats in the Southern Ocean: Implications for seasonal successions and
1339 particle export. *Journal of Geophysical Research: Oceans*, *122*(10), pp.8278-8292.

1340 Revilla, M., Alexander, J., and Glibert, P.M., (2005). Urea analysis in coastal waters: comparison of enzymatic and direct
1341 methods. *Limnology and Oceanography: Methods*, *3*(7), pp.290-299.

1342 Richardson, T.L. and Jackson, G.A., (2007). Small phytoplankton and carbon export from the surface ocean. *Science*,
1343 315(5813), pp.838-840.

https://doi.org/10.5194/bg-2021-149
Preprint. Discussion started: 10 June 2021

1344 Rintoul, S.R., and Trull, T.W., (2001). Seasonal evolution of the mixed layer in the Subantarctic Zone south of Australia.
1345 *Journal of Geophysical Research: Oceans*, *106*(C12), pp.31447-31462.

1346 Robinson, R.S., Jones, C.A., Kelly, R.P., Love, A., Closset, I., Rafter, P.A. and Brzezinski, M., (2020). A Test of the
1347 Diatom-Bound Paleoproxy: Tracing the Isotopic Composition of Nutrient-Nitrogen Into Southern Ocean Particles and
1348 Sediments. *Global Biogeochemical Cycles*, 34(10), p.e2019GB006508.

1349 Rodrigues, R.M., and Williams, P.J.L.B., (2001). Heterotrophic bacterial utilization of nitrogenous and nonnitrogenous
1350 substrates, determined from ammonia and oxygen fluxes. *Limnology and Oceanography*, 46(7), pp.1675-1683.

1351 Sallée, J.B., Speer, K.G. and Rintoul, S.R., (2010). Zonally asymmetric response of the Southern Ocean mixed-layer depth
1352 to the Southern Annular Mode. *Nature Geoscience*, 3(4), pp.273-279.

1353 Sambrotto, R.N. and Mace, B.J., (2000). Coupling of biological and physical regimes across the Antarctic Polar Front as
1354 reflected by nitrogen production and recycling. *Deep Sea Research Part II: Topical Studies in Oceanography*, 47(15-16),
1355 pp.3339-3367.

1356 Sarmiento, J. L., Gruber, N., Brzezinski, M. A., and Dunne, J. P. (2004). High-latitude controls of thermocline nutrients
1357 and low latitude biological productivity. *Nature*, *427*(6969), pp.56–60.

1358 Savoye, N., Dehairs, F., Elskens, M., Cardinal, D., Kopczyńska, E.E., Trull, T.W., Wright, S., Baeyens, W., and Griffiths,
1359 F.B., (2004). Regional variation of spring N-uptake and new production in the Southern Ocean. *Geophysical Research*
1360 *Letters*, 31(3).

1361 Schaafsma, F. L., Cherel, Y., Flores, H., van Franeker, J. A., Lea, M. A., Raymond, B., and van de Putte, A. P. (2018).
1362 Review: the energetic value of zooplankton and nekton species of the Southern Ocean. *Marine Biology*, 165(8), pp. 1–35.

1363 Scharek, R., Smetacek, V., Fahrbach, E., Gordon, L.I., Rohardt, G., and Moore, S., (1994). The transition from winter to
1364 early spring in the eastern Weddell Sea, Antarctica: plankton biomass and composition in relation to hydrography and
1365 nutrients. *Deep Sea Research Part I: Oceanographic Research Papers*, *41*(8), pp.1231-1250.

1366 Schön, G. H., and Engel, H. (1962). Der Einflußdes Lichtes auf Nitrosomonas europaea Win. *Archiv Für Mikrobiologie*,
1367 *42*(4), pp.415–428.

1368 Sedwick, P. N., Bowie, A. R., and Trull, T. W. (2008). Dissolved iron in the Australian sector of the Southern Ocean
1369 (CLIVAR SR3 section): Meridional and seasonal trends. *Deep-Sea Research Part I: Oceanographic Research Papers*,
1370 *55*(8), pp.911–925.

1371 Semeneh, M., Dehairs, F., Elskens, M., Baumann, M. E. M., Kopczynska, E. E., Lancelot, C., and Goeyens, L. (1998).
1372 Nitrogen uptake regime and phytoplankton community structure in the Atlantic and Indian sectors of the Southern Ocean.
1373 *Journal of Marine Systems*, *17*(1–4), pp.159–177.

1374 Serebrennikova, Y. M., and Fanning, K. A. (2004). Nutrients in the Southern Ocean GLOBEC region: Variations, water
1375 circulation, and cycling. *Deep-Sea Research Part II: Topical Studies in Oceanography*, *51*(17–19), pp.1981–2002.

1376 Shadwick, E.H., Trull, T.W., Tilbrook, B., Sutton, A.J., Schulz, E., and Sabine, C.L., (2015). Seasonality of biological and
1377 physical controls on surface ocean CO2 from hourly observations at the Southern Ocean Time Series site south of
1378 Australia. *Global Biogeochemical Cycles*, *29*(2), pp.223-238.

1379 Shafiee, R.T., Snow, J.T., Zhang, Q., and Rickaby, R.E., (2019). Iron requirements and uptake strategies of the globally
1380 abundant marine ammonia-oxidising archaeon, Nitrosopumilus maritimus SCM1. *The ISME joumal*, *13*(9), pp.2295-
1381 2305.

1382 Sigman, D. M., Altabet, M. A., McCorkle, D. C., Francois, R., and Fischer, G. (1999). The $\delta^{15}N$ of nitrate in the southern
1383 ocean: Consumption of nitrate in surface waters. *Global Biogeochemical Cycles*, *13*(4), pp.1149–1166.

1384 Sigman, D.M. and Boyle, E.A., (2000). Glacial/interglacial variations in atmospheric carbon dioxide. *Nature*, *407*(6806),
1385 pp.859-869.

1386 Sipler, R.E. and Bronk, D.A., (2015). Dynamics of dissolved organic nitrogen. *Biogeochemistry of marine dissolved*
1387 *organic matte*r, pp.127-232.

1388 Smart, S. M., Fawcett, S. E., Thomalla, S. J., Weigand, M. A., Reason, C. J. C., and Sigman, D. M. (2015). Isotopic
1389 evidence for nitrification in the Antarctic winter mixed layer. *Global Biogeochemical Cycles*, *29*(4), 427–445.

1390 Smart, S.M., Fawcett, S.E., Ren, H., Schiebel, R., Tompkins, E.M., Martínez-García, A., Stirnimann, L., Roychoudhury,
1391 A., Haug, G.H. and Sigman, D.M., (2020). The Nitrogen Isotopic Composition of Tissue and Shell-Bound Organic Matter
1392 of Planktic Foraminifera in Southern Ocean Surface Waters. *Geochemistry, Geophysics, Geosystems*, 21(2),
1393 p.e2019GC008440.

1394 Smith, J. M., Chavez, F. P., and Francis, C. A. (2014). Ammonium Uptake by Phytoplankton Regulates Nitrification in the
1395 Sunlit Ocean. *PLoS ONE*, *9*(9), e108173.

1396 Smith Jr, W.O. and Harrison, W.G., (1991). New production in polar regions: the role of environmental controls. *Deep*
1397 *Sea Research Part A. Oceanographic Research Papers*, 38(12), pp.1463-1479.

1398 Smith Jr, W.O. and Lancelot, C., (2004). Bottom-up versus top-down control in phytoplankton of the Southern
1399 Ocean. *Antarctic Science*, *16*(4), p.531.

https://doi.org/10.5194/bg-2021-149
Preprint. Discussion started: 10 June 2021

1400 Smith Jr, W.O., Marra, J., Hiscock, M.R. and Barber, R.T., (2000). The seasonal cycle of phytoplankton biomass and
1401 primary productivity in the Ross Sea, Antarctica. *Deep Sea Research Part II: Topical Studies in Oceanography*, *47*(15-
1402 16), pp.3119-3140.

1403 Soares, M.A., Bhaskar, P.V., Naik, R.K., Dessai, D., George, J., Tiwari, M. and Anilkumar, N., (2015). Latitudinal δ13C
1404 and δ15N variations in particulate organic matter (POM) in surface waters from the Indian ocean sector of Southern Ocean
1405 and the Tropical Indian Ocean in 2012. *Deep Sea Research Part II: Topical Studies in Oceanography*, *118*, pp.186-196.

1406 Sokolov, S. and Rintoul, S.R., (2007). On the relationship between fronts of the Antarctic Circumpolar Current and
1407 surface chlorophyll concentrations in the Southern Ocean. *Journal of Geophysical Research: Oceans*, *112*(C7).

1408 Sosik, H.M. and Olson, R.J., (2002). Phytoplankton and iron limitation of photosynthetic efficiency in the Southern Ocean
1409 during late summer. *Deep Sea Research Part I: Oceanographic Research Papers*, *49*(7), pp.1195-1216.

1410 Steinberg, D.K. and Saba, G.K., (2008). Nitrogen consumption and metabolism in marine zooplankton. In *Nitrogen in the*
1411 *marine environment* (pp. 1135-1196). Elsevier Inc.

1412 Strickland, J.D.H. and Parsons, T.R., (1972). A practical handbook of seawater analysis.

1413 Strzepek, R.F., Boyd, P.W. and Sunda, W.G., (2019). Photosynthetic adaptation to low iron, light, and temperature in
1414 Southern Ocean phytoplankton. *Proceedings of the National Academy of Sciences*, 116(10), pp.4388-4393.

1415 Sunda, W.G. and Huntsman, S.A., (1997). Interrelated influence of iron, light and cell size on marine phytoplankton
1416 growth. Nature, 390(6658), pp.389-392.

1417 Tagliabue, A., Mtshali, T., Aumont, O., Bowie, A.R., Klunder, M.B., Roychoudhury, A.N. and Swart, S., (2012). A global
1418 compilation of dissolved iron measurements: focus on distributions and processes in the Southern Ocean. *Biogeosciences*,
1419 9(6), pp.2333-2349.

1420 Tagliabue, A., Sallée, J.B., Bowie, A.R., Lévy, M., Swart, S., and Boyd, P.W., (2014). Surface-water iron supplies in the
1421 Southern Ocean sustained by deep winter mixing. *Nature Geoscience*, *7*(4), pp.314-320.

1422 Takao, S., Hirawake, T., Wright, S.W., and Suzuki, K., (2012). Variations of net primary productivity and phytoplankton
1423 community composition in the Indian sector of the Southern Ocean as estimated from ocean color remote sensing
1424 data. *Biogeosciences*, *9*(10), pp.3875-3890.

1425 Talmy, D., Martiny, A.C., Hill, C., Hickman, A.E., and Follows, M.J., (2016). Microzooplankton regulation of surface
1426 ocean POC: PON ratios. *Global Biogeochemical Cycles*, 30(2), pp.311-332.

1427 Tevlin, A.G., and Murphy, J.G., (2019). Atmospheric Ammonia: Measurements, Modeling, and Chemistry–Climate
1428 Interactions. *Advances In Atmospheric Chemistry-Volume 2: Organic Oxidation And Multiphase Chemistry*, *2*, p.1.

1429 Thomalla, S.J., Waldron, H.N., Lucas, M.I., Read, J.F., Ansorge, I.J., and Pakhomov, E., (2011). Phytoplankton
1430 distribution and nitrogen dynamics in the southwest indian subtropical gyre and Southern Ocean waters. *Ocean Science*,
1431 *7*(1), pp.113-127.

1432 Timmermans, K.R., Stolte, W. and De Baar, H.J.W., (1994). Iron-mediated effects on nitrate reductase in marine
1433 phytoplankton. *Marine Biology*, *121*(2), pp.389-396.

1434 Timmermans, K.R., Van Leeuwe, M.A., De Jong, J.T.M., McKay, R.M.L., Nolting, R.F., Witte, H.J., Van Ooyen, J.,
1435 Swagerman, M.J.W., Kloosterhuis, H. and De Baar, H.J., (1998). Iron stress in the Pacific region of the Southern Ocean:
1436 evidence from enrichment bioassays. *Marine Ecology Progress Series*, *166*, pp.27-41.

1437 Tolar, B.B., Ross, M.J., Wallsgrove, N.J., Liu, Q., Aluwihare, L.I., Popp, B.N., and Hollibaugh, J.T. (2016). Contribution
1438 of ammonia oxidation to chemoautotrophy in Antarctic coastal waters. *ISME Journal*, *10*(11), pp.2605–2619.

1439 Tréguer, P. and Jacques, G., (1992). Review Dynamics of nutrients and phytoplankton, and fluxes of carbon, nitrogen and
1440 silicon in the Antarctic Ocean. In *Weddell Sea Ecology* (pp. 149-162). Springer, Berlin, Heidelberg.

1441 Treibergs, L.A., Fawcett, S.E., Lomas, M.W. and Sigman, D.M., (2014). Nitrogen isotopic response of prokaryotic and
1442 eukaryotic phytoplankton to nitrate availability in Sargasso Sea surface waters. *Limnology and Oceanography*, 59(3),
1443 pp.972-985.

1444 Trull, T.W., Davies, D. and Casciotti, K., (2008). Insights into nutrient assimilation and export in naturally iron-fertilized
1445 waters of the Southern Ocean from nitrogen, carbon and oxygen isotopes. *Deep Sea Research Part II: Topical Studies in*
1446 *Oceanography*, *55*(5-7), pp.820-840.

1447 Utermöhl, H., (1958). Zur vervollkommnung der quantitativen phytoplankton-methodik: mit 1 Tabelle und 15
1448 abbildungen im Text und auf 1 Tafel. *Internationale Vereinigung für theoretische und angewandte Limnologie:*
1449 *Mitteilungen*, *9*(1), pp.1-38.

1450 Vaulot, D., Courties, C. and Partensky, F., (1989). A simple method to preserve oceanic phytoplankton for flow
1451 cytometric analyses. *Cytometry: The Journal of the International Society for Analytical Cytology*, *10*(5), pp.629-635.

1452 Venkataramana, V., Anilkumar, N., Naik, R.K., Mishra, R.K. and Sabu, P., (2019). Temperature and phytoplankton size
1453 class biomass drives the zooplankton food web dynamics in the Indian Ocean sector of the Southern Ocean. *Polar*
1454 *Biology*, *42*(4), pp.823-829.

https://doi.org/10.5194/bg-2021-149
Preprint. Discussion started: 10 June 2021

1455 Viljoen, J.J., Weir, I., Fietz, S., Cloete, R., Loock, J., Philibert, R. and Roychoudhury, A.N., (2019). Links between the
1456 phytoplankton community composition and trace metal distribution in summer surface waters of the Atlantic southern
1457 ocean. *Frontiers in Marine Science*, *6*, p.295.

1458 Wadley, M.R., Jickells, T.D., and Heywood, K.J., (2014). The role of iron sources and transport for Southern Ocean
1459 productivity. *Deep Sea Research Part I: Oceanographic Research Papers*, *87*, pp.82-94.

1460 Wan, X.S., Sheng, H.X., Dai, M., Zhang, Y., Shi, D., Trull, T.W., Zhu, Y., Lomas, M.W. and Kao, S.J., (2018). Ambient
1461 nitrate switches the ammonium consumption pathway in the euphotic ocean. *Nature communications*, *9*(1), pp.1-9.

1462 Ward, B. B. (1985). Light and substrate concentration relationships with marine ammonium assimilation and oxidation
1463 rates. *Marine Chemistry*, *16*(4), pp.301–316.

1464 Ward, B.B., (2005). Temporal variability in nitrification rates and related biogeochemical factors in Monterey Bay,
1465 California, USA. *Marine Ecology Progress Series*, *292*, pp.97-109.

1466 Weber, L.H. and El-Sayed, S.Z., (1987). Contributions of the net, nano-and picoplankton to the phytoplankton standing
1467 crop and primary productivity in the Southern Ocean. *Journal of Plankton Research*, *9*(5), pp.973-994.

1468 Wei, T., and Simko, V., (2017). R package "corrplot": Visualization of a Correlation Matrix (Version 0.84). Available
1469 from https://github.com/taiyun/corrplot

1470 Weir, I., Fawcett, S., Smith, S., Walker, D., Bornman, T. and Fietz, S., (2020). Winter biogenic silica and diatom
1471 distributions in the Indian sector of the Southern Ocean. *Deep Sea Research Part I: Oceanographic Research Papers*, *166*,
1472 p.103421.

1473 Welschmeyer, N.A., (1994). Fluorometric analysis of chlorophyll a in the presence of chlorophyll b and
1474 pheopigments. *Limnology and Oceanography*, *39*(8), pp.1985-1992.

1475 Wickham H (2016). *ggplot2: Elegant Graphics for Data Analysis*. Springer-Verlag New York. ISBN 978-3-319-24277-
1476 4, https://ggplot2.tidyverse.org.

1477 Xu, G., Chen, L., Zhang, M., Zhang, Y., Wang, J. and Lin, Q., (2019). Year-round records of bulk aerosol composition
1478 over the Zhongshan Station, Coastal East Antarctica. *Air Quality, Atmosphere & Health*, 12(3), pp.271-288.

1479 Yu G. (2019). shadowtext: Shadow Text Grob and Layer. R package version 0.0.7. https://CRAN.R-
1480 project.org/package=shadowtext

1481 Zakem, E. J., Al-Haj, A., Church, M. J., Van Dijken, G. L., Dutkiewicz, S., Foster, S. Q., Fulweiler, R. W., Mills, M. M.,
1482 and Follows, M. J. (2018). Ecological control of nitrite in the upper ocean. *Nature Communications*, *9*(1), pp.1–13.

1483 Zhou, J., Delille, B., Kaartokallio, H., Kattner, G., Kuosa, H., Tison, J.L., Autio, R., Dieckmann, G.S., Evers, K.U.,
1484 Jørgensen, L. and Kennedy, H., (2014). Physical and bacterial controls on inorganic nutrients and dissolved organic
1485 carbon during a sea ice growth and decay experiment. *Marine Chemistry*, 166, pp.59-69.

1486

1487 **Figure and Table Captions**

https://doi.org/10.5194/bg-2021-149
Preprint. Discussion started: 10 June 2021

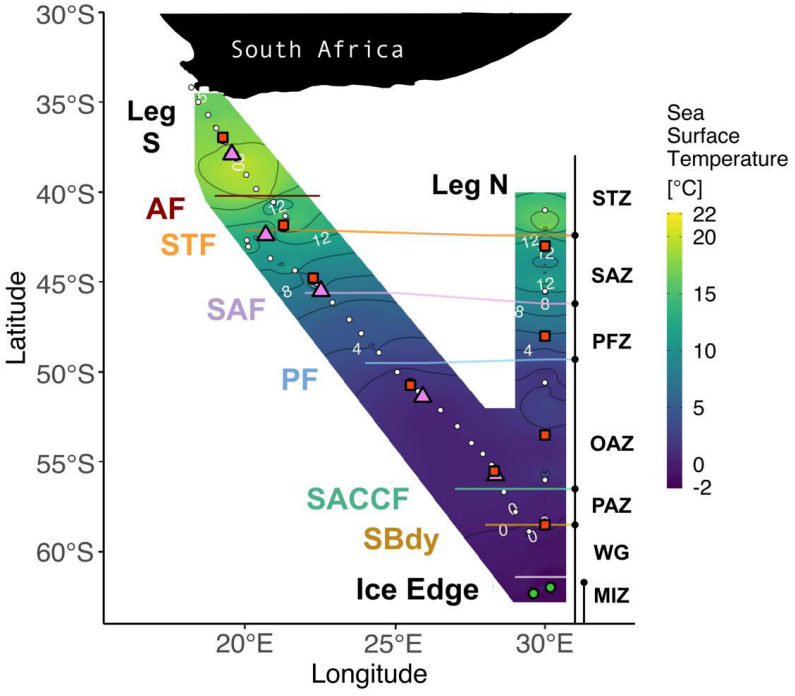

1488

1489 *Figure 1*: Winter 2017 cruise track overlaid on sea surface temperature (SST) measured by the hull-
1490 mounted thermosalinograph. The underway (Leg S) and CTD (Leg N) stations are indicated by white
1491 circles. Stations at which net primary production (NPP), nitrogen uptake, and ammonium oxidation
1492 experiments were conducted are denoted by red squares. The pink triangles indicate stations where only
1493 NPP experiments were conducted while the green circles show stations where only ammonium
1494 oxidation was measured. Solid lines indicate the positions of the fronts, identified using temperature and
1495 salinity, measurements. Abbreviations for fronts: AF – Agulhas Front (~40.2°S); STF – Subtropical
1496 Front (~42.1°S); SAF – Subantarctic Front (~45.6°S); PF – Polar Front (~49.5°S); SACCF –
1497 Southern Antarctic Circumpolar Current Front (~56.5°S); SBDY – Southern Boundary (~58.5°S).
1498 Abbreviations for zones: STZ – Subtropical Zone; SAZ – Subantarctic Zone; PFZ – Polar Frontal Zone;
1499 OAZ – Open Antarctic Zone; PAZ – Polar Antarctic Zone; WG – Weddell Gyre; MIZ – Marginal Ice
1500 Zone. Figure produced using the package ggplot2 (Wickham, 2016).

1501 *Table 1*: Mean (± 1 SD) of surface ocean POC, PON, chl-a, and nutrient concentrations, cell
1502 abundances, and nutrient uptake rates measured in each zone of the Southern Ocean in winter 2017.
1503 Where no SD is given, only one sample was measured. ND – no data available. Abbreviations as in
1504 Figure 1.

1505

https://doi.org/10.5194/bg-2021-149
Preprint. Discussion started: 10 June 2021

	STZ	SAZ	PFZ	OAZ	PAZ
NH_4^+ (µM)	0.08±0.03	0.06±0.01	0.42±0.01	0.52±0.01	0.58±0.01
PO_4^{3-} (µM)	0.44±0.07	0.90±0.06	1.59±0.1	2.00±0.13	1.99±0.09
NO_3^- (µM)	3.6±0.2	10.5±0.5	21.5±0.2	26.7±0.4	27.5±0.4
$Si(OH)_4$ (µM)	2.6±0.1	2.5±1.8	6.6±0.1	40.3±0.5	45.0±0.8
NO_2^- (µM)	0.15±0.02	0.13±0.02	0.17±0.02	0.19±0.01	0.21±0.02
Urea (µM)	0.23±0.04	0.11±0.04	0.26±0.08	0.24	0.21±0.03
chl-a (>0.3 µm) (µg L^{-1})	0.65±0.08	0.43±0.05	0.35±0.03	0.25±0.02	0.21±0.00
chl-a (>2.7 µm) (µg L^{-1})	0.50±0.05	0.30±0.04	0.24±0.02	0.18±0.02	0.17±0.02
chl-a (0.3-2.7 µm) (µg L^{-1})	0.15±0.1	0.13±0.07	0.11±0.04	0.06±0.03	0.04±0.02
chl-a (% of total of >2.7 µm)	77.5±13.9	73.1±10.9	69.8±8.7	76.7±11.3	80.1±8.5
POC (>0.3 µm) (µM)	4.38±6.67	3.4±0.43	3.23±0.26	3.43±0.48	3.47+0.22
POC (>2.7 µm) (µM)	2.63±0.51	2.59±0.43	1.87±1.22	1.92±0.36	4.64
PON (>0.3 µm) (µM)	0.61±0.19	0.48±0.08	0.44±0.08	0.50±0.14	0.54±0.09
PON (>2.7 µm) (µM)	0.26±0.06	0.28±0.06	0.24±0.28	0.22±0.12	0.38±0.02
POC (% of total of >2.7µm)	79.70±33.25	79.58±24.17	50.89±65.32	77.19±28.10	143.02
PON (% of total of >2.7µm)	69.04±43.26	67.12±29.47	53.8±121.41	66.98±49.74	ND
POC:chl-a (g g^{-1})	103.0±22.1	102.5±14.4	122.5±11	234.1±29.2	219.3±1.0
POC:PON (M/M)	7.81±6.49	6.90±1.25	7.13±0.71	6.72±1.62	5.80±3.75
δ^{15}N-PON	1.4±0.9	1.2±1.0	0.3±0.5	-1.3±0.5	-1.3±0.4
NPP (>0.3 µm) (nM day^{-1})	497.1±42.4	277.5±21.3	289.7±19.2	85.3±26.1	27.7±0.2
NPP (>2.7 µm) (nM day^{-1})	384.7±29.7	178.2±23.4	193.5	49.6±5.0	ND
ρNH_4^+ (>0.3 µm) (nM day^{-1})	5.7±0.8	8.9±1.1	12.9±0.4	4.8±0.1	3.0±0.8
ρNH_4^+ (>2.7 µm) (nM day^{-1})	4.0±1.1	4.1±1.2	4.2±4.7	3.1±0.4	ND
ρNO_3^- (>0.3 µm) (nM day^{-1})	4.1±0.4	11.5±1.4	5.9±1	3.6±0.4	3.7±1.8
ρNO_3^- (>2.7 µm) (nM day^{-1})	3.4±0.3	6.6±0.4	4.3±0.4	2.6±0.8	2.7±1.2
ρUrea (>0.3 µm) (nM day^{-1})	7.5±0.6	6.9±0.3	6.5±1.0	2.1±0.3	0.6±0.01
ρUrea (>2.7 µm) (nM day^{-1})	4.9±0.3	3.8±0.2	4.0±0.6	1.3±0.2	0.7±0.4
NH_4^+ox (nM day^{-1})	9.3±0.5	12.9±0.6	11.1	17.7±0.6	14.3±1.0
Total microplankton (cells mL^{-1})	13±11	5±3	9±3	6±6	4±2
Centric diatoms (cells mL^{-1})	<1	<1	<1	<1	1±2
Pennate diatoms (cells mL^{-1})	2±4	<1	2±1	2±3	<1
Dinoflagellates (cells mL^{-1})	7±6	4±0	6±2	3±2	2±0
Micro-zooplankton (cells mL^{-1})	4±3	<1	2±2	1±2	<1
Nanoeukaryotes (cells mL^{-1})	ND	2.2±1.4 E+03	1.5±0.7 E+03	1.6±0.7 E+03	1.4E+03
Picoeukaryotes (cells mL^{-1})	ND	4.5±2.9 E+03	4.9±3.7 E+03	1.5±0.5 E+03	8E+02
Synechococcus (cells mL^{-1})	ND	3.8±1.8 E+03	2.3±1.1 E+03	1.4±0.2 E+03	1E+03
Small heterotrophs (cells mL^{-1})	ND	4.5±3.2 E+03	2.3±1.2 E+03	2.1±2.3 E+03	3.2E+03
Detritus (particles mL^{-1})	ND	38.2±14.9 E+03	63.8±42.9 E+03	25.7±18.6 E+03	2.57E+04
NH_4^+ : NO_2^-	0.62±0.17	0.44±0.3	2.53±0.10	2.88±0.07	2.79±0.07

1506

https://doi.org/10.5194/bg-2021-149
Preprint. Discussion started: 10 June 2021

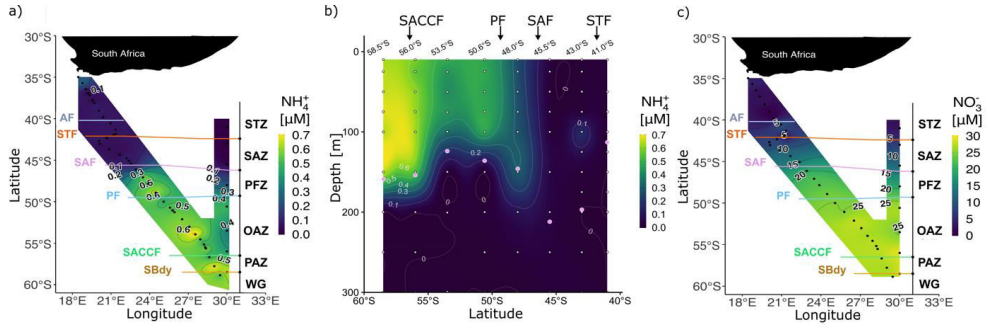

1507

1508 *Figure 2*: Concentrations of dissolved ammonium (NH_4^+) a) at the surface for Legs S and N and b) with
1509 depth for Leg N, and c) concentrations of nitrate (NO_3^-) at the surface for Legs S and N. Pink circles in
1510 panel b show the mixed layer depth at each CTD station. Abbreviations as in Figure 1. Figure produced
1511 using the package ggplot2 (Wickham, 2016).

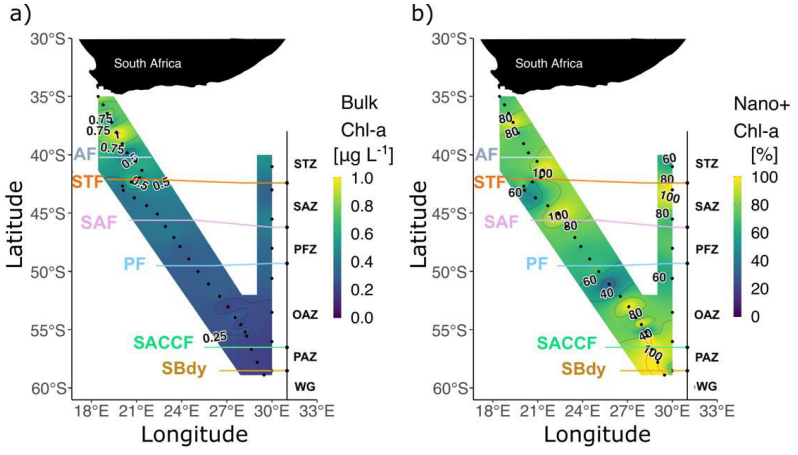

1512

1513 *Figure 3*: a) Bulk (>0.3 µm) chlorophyll-a (chl-a) concentrations and b) proportion of chlorophyll-a in
1514 the >2.7 µm size fraction (i.e., nanophytoplankton; % of total bulk chl-a) at the surface for Legs S and
1515 N. Abbreviations as in Figure 1. Figure produced using the package ggplot2 (Wickham, 2016).

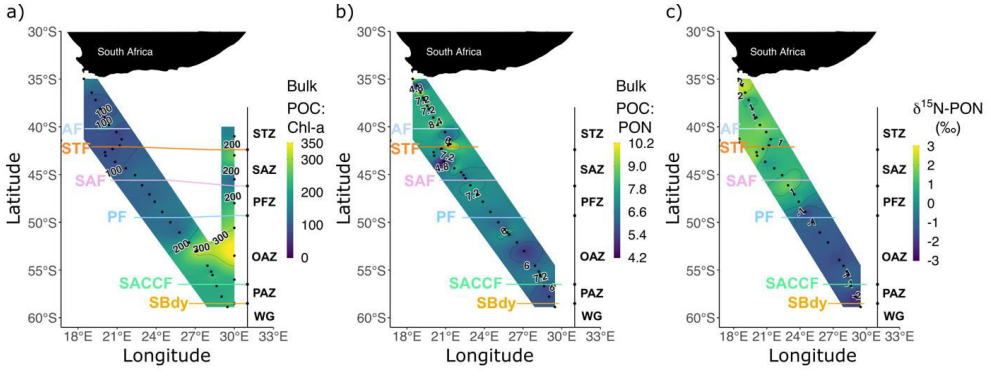

1516

https://doi.org/10.5194/bg-2021-149
Preprint. Discussion started: 10 June 2021

1517 *Figure 4*: a) Bulk (>0.3 µm) POC to chlorophyll-a ratio (weight:weight) at the surface for Legs S and N,
1518 and b) bulk POC to PON (molar) ratio and c) δ^{15}N-PON at the surface for Leg S. The stations nearest
1519 South Africa at which biomass concentrations were extremely high have been excluded from panels b
1520 and c. Abbreviations as in Figure 1. Figure produced using the package ggplot2 (Wickham, 2016).

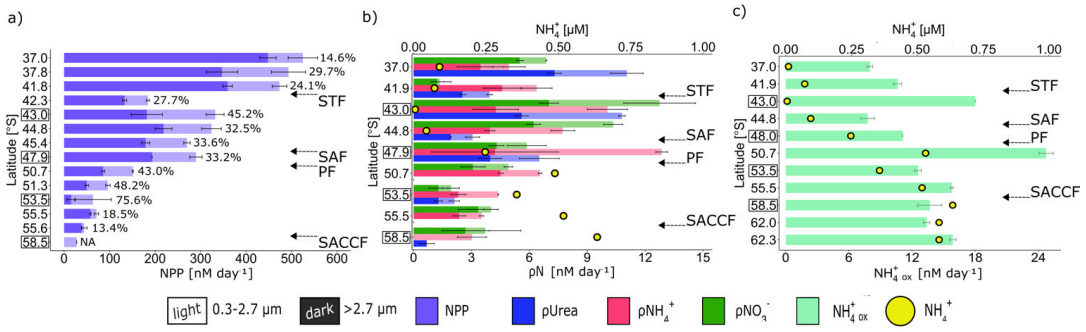

1521

1522 *Figure 5*: Surface rates of a) net primary production (NPP; ρC) for two plankton size fractions (>0.3 and
1523 >2.7 µm); b) urea, ammonium (NH_4^+), and nitrate (NO_3^-) uptake for two plankton size fractions (>2.7
1524 µm overlaid on >0.3 µm), and c) NH_4^+ oxidation. Error bars indicate ±1 standard deviation of duplicate
1525 experiments. The percentage of total NPP attributable to the 0.3-2.7 µm size fraction is written next to
1526 each bar in panel a. NPP and NH_4^+ uptake were not measured for the >2.7 µm size fraction at 58.5°S,
1527 and urea uptake was not measured at 50.7°S and 55.5°S. On panels b and c, the surface NH_4^+
1528 concentration at each station is shown by the yellow circles. Leg N stations (i.e., at which samples were
1529 collected from Niskin bottles fired at 10 m) are indicated by the open square around the station latitude.
1530 Abbreviations as in Figure 1. Figure produced using the package ggplot2 (Wickham, 2016).

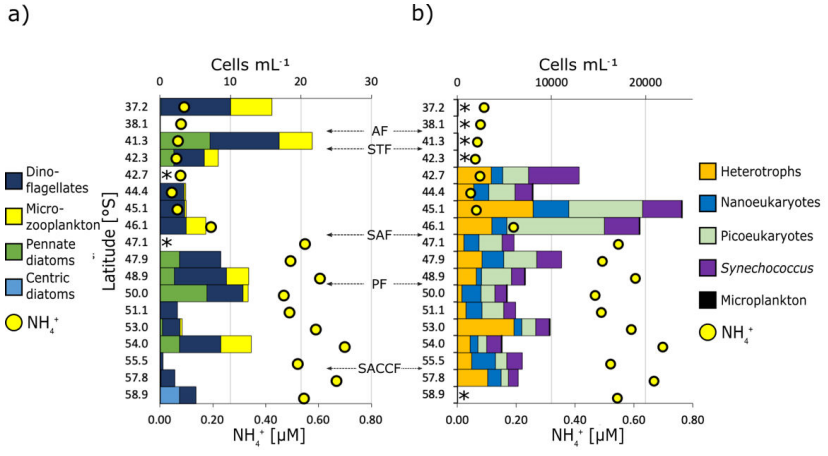

1531

1532 *Figure 6*: Surface community composition for a) plankton >5-10 µm (enumerated by microscopy) and
1533 b) the total community <15 µm (enumerated by flow cytometry). The surface NH_4^+ concentration at
1534 each station is shown by the yellow circles. * indicates stations at which no measurements were made.
1535 The abundance axis in panel b is 10^3-times greater than the abundances shown in panel a. The fronts are
1536 indicated on panel a with abbreviations as in Figure 1.

https://doi.org/10.5194/bg-2021-149
Preprint. Discussion started: 10 June 2021

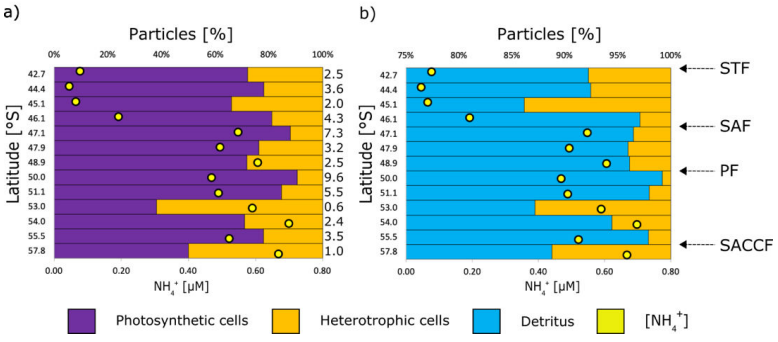

1537

1538 *Figure 7*: Relative abundances of a) total photosynthetic versus heterotrophic cells and b) detritus
1539 (DNA-negative) versus heterotrophic cells at the surface for Leg S. The surface NH_4^+ concentration is
1540 indicated by the yellow dots. The values shown on the right side of panel a are the heterotrophic-to-
1541 photosynthetic cell ratios. The upper x-axis in panel b begins at 75% in order to highlight the (much
1542 smaller) heterotrophic contribution to the summed detrital + heterotrophic particles. Abbreviations as in
1543 Figure 1.

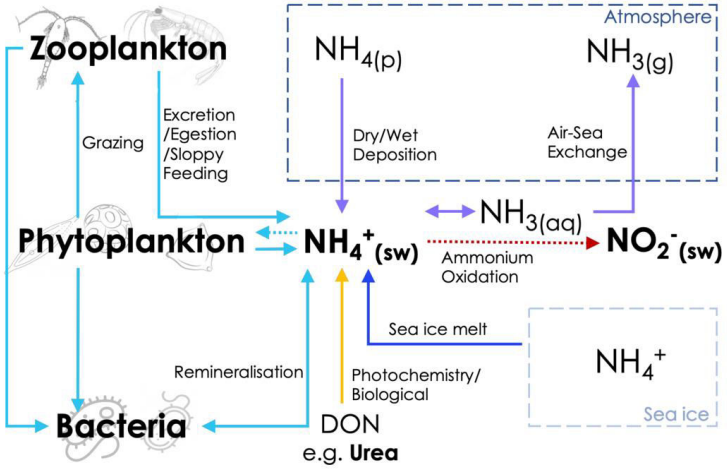

1544

1545 *Figure 8*: Schematic of the possible mixed-layer NH_4^+ consumption and production pathways. Bold text
1546 indicates components of the NH_4^+ cycle that were directly measured (seawater concentrations of NH_4^+,
1547 NO_2^-, and urea; phytoplankton and microzooplankton cell abundances) or inferred (bacterial NH_4^+
1548 remineralization) in this study. Dotted lines indicate processes for which we have rate measurements
1549 (phytoplankton uptake of NH_4^+; oxidation of NH_4^+ to NO_2^-). Dashed-line boxes represent the
1550 atmosphere and sea-ice, with all other processes occurring in the ocean. DON – dissolved organic
1551 nitrogen; $NH_{3(aq)}$ – aqueous (seawater) ammonia; $NH_{4(p)}$ – ammonium aerosols (including ammonium
1552 sulphate, ammonium bisulphate, and ammonium nitrate); $NH_{3(g)}$ – ammonia gas.

https://doi.org/10.5194/bg-2021-149
Preprint. Discussion started: 10 June 2021

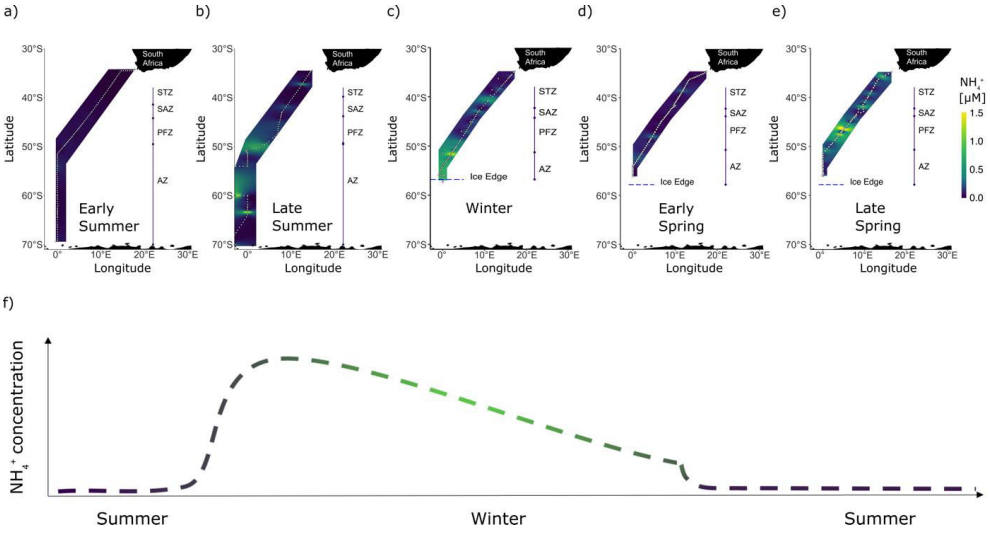

Figure 9: Surface concentrations of NH_4^+ across the Atlantic sector of the Southern Ocean measured between December 2018 and November 2019. Five unique transects additional to the winter 2017 dataset are shown: a) early summer 2018, b) late summer 2019, c) winter 2019, d) early spring 2019, and e) late spring 2019. f) Proposed seasonal cycle of NH_4^+ concentrations in the mixed layer for the waters south of the Subantarctic Front. The colour gradient in panel f indicates the transition period between winter and summer. Panels a and b cover a latitudinal extent of 30-70°S, while panels c-e cover 30-60°S due to the presence of sea-ice. Early- and late summer data were collected during the SANAE 58 Relief Voyage (6 December 2018 to 15 March 2019; VOY035); winter data were collected during the SCALE 2019 (www.scale.org.za) winter cruise to the MIZ (18 July to 12 August 2019; VOY039); and spring data were collected during the SCALE 2019 spring cruise to the MIZ (12 October to 20 November 2019; VOY040). All sampling was conducted onboard the R/V *SA Agulhas II*. Abbreviations as in Figure 1, with AZ referring to the combined OAZ and PAZ. Figure produced using the package ggplot2 (Wickham, 2016).